Global Journal of Pure and Applied Mathematics.
ISSN 0973-1768 Volume 12, Number 2 (2016), pp. 1337-1374

http://www.ripublication.com

Mathematical analysis for unsteady dispersion of solutes in blood stream-A comparative study

D. S. Sankar[a]*, Nurul Aini Jaafar[b], Yazariah Yatim[c]

[a]Engineering Mathematics Unit, Faculty of Engineering, Universiti Teknologi Brunei, Jalan Tungku Link, Gadong BE 1410, Brunei Darussalam
[b, c]School of Mathematical Sciences, Universiti Sains Malaysia, 11800 USM, Penang, Malaysia
**Corresponding author:*

Abstract

The unsteady dispersion of solutes in blood flow through (i) circular pipe and (ii) channel between parallel plates is analyzed mathematically, treating blood as Herschel-Bulkley fluid. Derivative series expansion method is applied to solve the resulting convective diffusion equation. It is found that the dispersion coefficient, relative effective diffusivity and magnitude of the dispersion function decrease considerably with the increase of the yield stress of blood, when the solute disperses in the flow through pipe/channel. The aforesaid flow measurements are considerably higher when the solute disperses in the flow through pipe than when it disperses in the flow through channel. Estimates of the percentage of decrease in the dispersion coefficient and effective axial diffusivity are significantly lower when the solute disperses in Herschel-Bulkley fluid than when it disperses in Casson fluid and these estimates are lower when the solute disperses in pipe than when it disperses in channel.

Keywords: Unsteady dispersion of solutes; Blood flow; Flow in pipe/channel; Herschel-Bulkley fluid; Relative diffusivity; Effective axial diffusivity

1. Introduction

The shear augmented dispersion of solutes in fluid flow (solvent) is an important physical phenomena and is an upcoming research topic which attracted researchers from various branches of science due to its abundant applications in the fields of biophysics, physiological fluid dynamics, biomechanics, bio-medical engineering,

chemical engineering, clinical biology, environmental science etc [1-3]. Some specific applications of this research area are the mixing and transport of drugs in physiological systems, dispersion of gaseous tracer in chemical engineering, transport of pollutants in the environment, chromatographic separations in chemical engineering [4, 5]. The basic theory for this dispersion process is the spreading of the passive species (solute) in the flowing fluid (solvent) by the combined action of molecular diffusion and non-uniform velocity distribution [6, 7].

Taylor [8] was the first to investigate on this research topic and in his seminal contribution, he reported that, when a bolus of solute is injected into a solvent (flowing fluid) which undergoes steady motion in a straight pipe, due to the combined action of the lateral molecular diffusion and variation in the fluid's velocity over the cross section, the solute disperses diffusively with the effective molecular diffusivity $D_{eff} = a^2 u_m^2 / 48 D_m$, where a is the radius of the pipe, u_m is the mean velocity and D_m is the molecular diffusivity. Aris [9] used the method of moments to investigate on the solutes dispersion process and commented that the Taylor's dispersion theory is valid only when $D_{eff} >> D_m$ and corrected the Taylor's formula for effective molecular diffusivity as $D_{eff} = D_m + a^2 u_m^2 / 48 D_m$. Ananthakrishnan et al. [10] analyzed the solutes dispersion in laminar fluid flow by considering diffusion in both radial and axial directions and propounded that the Taylor-Aris dispersion theory is valid only when the time after the injection of the solute exceeds $0.5\left(a^2 / D_m\right)$.

Gill [11] used the method of series expansion about the mean concentration (in terms of derivatives of mean concentrations) for solving the convective diffusion equation. Gill and Sankarasubramanian [12] extended this to the generalized dispersion model for the unsteady convective diffusion of solutes in laminar flow in circular pipe and obtained series solution to the problem. Sankarasubramanian and Gill [13] further extended this to incorporate the interphase transport effects and found out that the three effective transport coefficients, namely the exchange, convection and dispersion coefficients were all influenced by the interphase transport. Sharp [14] applied the Taylor-Aris dispersion theory to study the steady dispersion of solutes in Casson fluid flow through pipe and channel and pointed out that the relative diffusivity is strongly dependent on the yield stress of the solvent fluid. Phillips et al. [15] discussed the application of the dispersion of solutes in fluid flow to the transport of a soluble tracer substance through a wall layer consisting of a tube containing flowing fluid surrounded by a wall layer. Ramana et al. [16] analyzed the dispersion of solutes in a conduit, modeling the solvent as H-B fluid and used first order approximation to the constitutive equations of H-B fluid model for obtaining the flow quantities. Sankar et al. [17] mathematically analyzed the steady shear augmented dispersion of solutes in blood flow through pipe and channel, modeling blood as Herschel-Bulkley (H-B) model and mentioned that the effective axial diffusivity is higher when the solute disperses in pipe than in channel.

Blood shows anomalous behavior when it flows through arteries of different diameters. When it flows through larger arteries (arteries diameter $> 300 \mu m$) at high shear rates, it shows Newtonian fluid's character, but, when it flows in narrow arteries

(arteries diameter $< 300\mu m$) at low shear rates, it exhibits remarkable non-Newtonian fluid's behavior [18-21]. Normal blood flow in arteries and veins is disturbed by the injection of solutes (medicines) in the blood stream and the non-Newtonian behavior of blood in narrow arteries affects the normal shear dispersion of solutes in the blood stream. Thus, it is important to study the changes caused by the non-Newtonian rheology of blood in narrow arteries to the dispersion of the solutes in blood stream. Casson and H-B fluids are some of the non-Newtonian fluid models with yield stress which are frequently used for blood flow modeling in narrow arteries at low shear rates. Some advantages of using H-B fluid rather than Casson fluid model for modeling blood flow in narrow arteries at low shear rates are mentioned below.

Scott Blair [22] propounded that the H-B fluid model is easier to explain in most cases and is more appropriate and more general for blood flow. Scott Blair and Spanner [23] reported that blood behaves like Casson fluid only at moderate shear rate in smaller diameter arteries, whereas, the behavior of blood at low shear rates flow in narrow arteries can be explained by H-B fluid and it can represent fairly closely what is occurring in blood when the yield stress is high. Chaturani and Ponnalagar Samy [24] pointed out that when blood flow in arteries of diameter 95 μm , blood behaves like H-B fluid rather than power-law and Bingham fluids. Iida [25] reports "the velocity profile in the arterioles having diameter less than $0.1mm$ are generally explained fairly by Casson and H-B fluid models. However, the velocity profiles in the arterioles whose diameters are less than $0.065mm$ do not conform to the Casson fluid model, but, can still be explained by H-B model". Hence, it is appropriate to model blood as H-B fluid model rather than Casson fluid model when it flows through smaller diameter arteries. Dash et al. [26] investigated the unsteady dispersion of solutes in the steady flow of Casson fluid in a conduit. Since H-B fluid model has several advantages over Casson fluid model (as mentioned above), it will be very useful to study the unsteady dispersion of solutes in the steady flow of H-B fluid. To the knowledge of the authors, the unsteady dispersion of solutes in the steady flow of blood through conduits, modeling blood as H-B fluid, has not been studied by anyone so far. Hence, in this paper, we have mathematically analyzed the unsteady dispersion of solutes in blood flow through narrow circular arteries, modeling blood as H-B fluid. Since, some clinical devices uses the blood flow through channel between parallel flat plates [14, 26, 27], we have also extended the study to the dispersion of solutes in blood flow through a channel between parallel flat plates. The layout of this paper is as follows.

Section 2 formulates the problem mathematically and then non-dimensionalizes the governing equations for flow in (i) circular pipe and (ii) channel between parallel flat plates and then solves them to obtain the expression for the physiologically important flow quantities such as normalized velocity, longitudinal diffusion coefficient, concentration of the fluid and the dispersion function. The effects of various parameters such as power-law index, time and yield stress on the aforesaid flow quantities are discussed through appropriate graphs in the results and discussion in Section 3. In Section 3, the results obtained for pipe flow analysis are compared with the results obtained for channel flow analysis and the results obtained for unsteady dispersion of solutes in H-B fluid flow are compared with the results obtained by

Dash et al. [26] for unsteady dispersion of solutes in Casson fluid flow. Some possible clinical applications of the present study are also given in Section 3. The main findings of this mathematical analysis are summarized in the concluding Section 4.

2. Mathematical formulation and solution methodology

Consider the laminar, steady, axisymmetric and fully developed unidirectional flow (in the axial direction) of blood (assumed as viscous incompressible fluid) through a (i) circular pipe and (ii) channel between parallel flat plates, treating blood as H-B fluid. The flow geometries in pipe and channel between parallel flat plates are depicted in Figs. 1a and 1b, respectively.

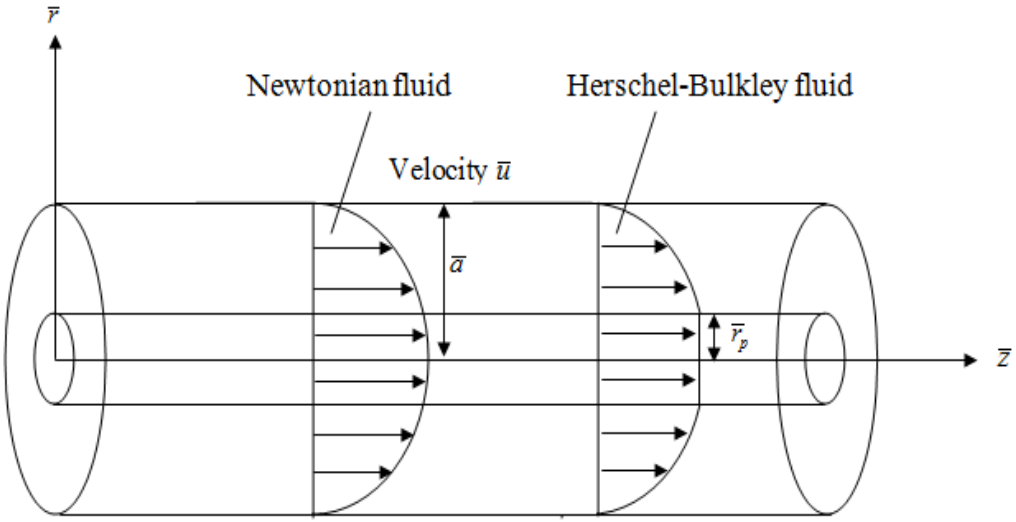

(a) Flow in a pipe.

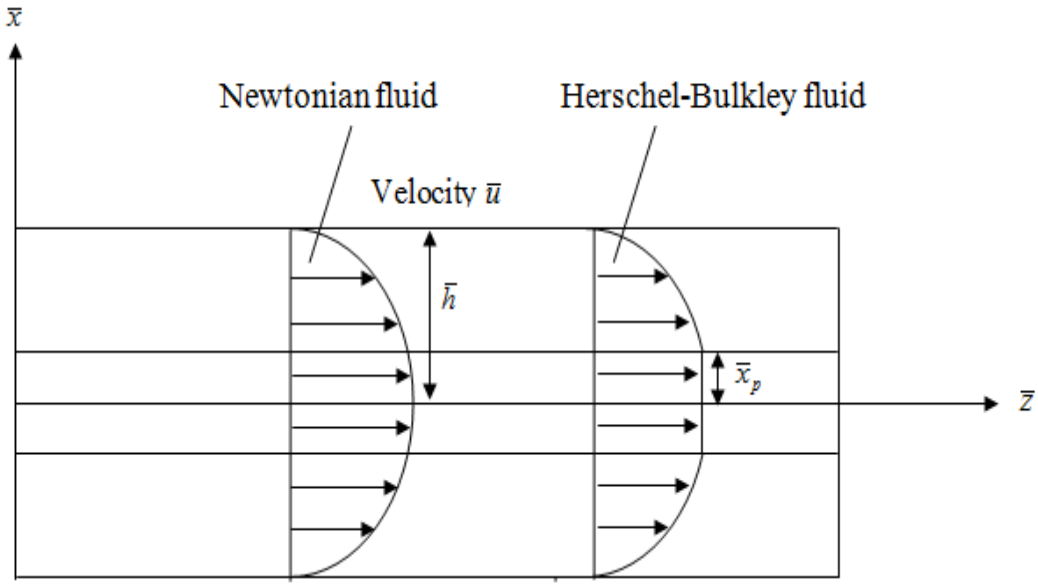

(b) Flow in a channel.

Figure 1: The geometry of the fluid flow in (a) pipe and (b) channel.

2.1 Flow in pipe

2.1.1 Governing equations

Consider the unsteady dispersion of a bolus of solute of initial length $\bar{z}_s$ units in a straight circular pipe of radius $\bar{a}$. Cylindrical polar coordinate system $(\bar{r},\bar{\psi},\bar{z})$ is used to analyze the flow in a pipe as shown in Fig. 1(a), where $\bar{r}$ and $\bar{z}$ are the coordinates in the radial and axial directions respectively, and $\bar{\psi}$ is the azimuthal angle. For the steady slow flow of viscous incompressible fluid, the axial and radial components of the momentum equations simplify to the following equations.

$$\frac{d\bar{p}}{d\bar{z}} = -\frac{1}{\bar{r}}\frac{d}{d\bar{r}}(\bar{r}\bar{\tau}) \tag{1}$$

$$\frac{d\bar{p}}{d\bar{r}} = 0 \tag{2}$$

where $\bar{p}$ is the pressure and $\bar{\tau}$ is the shear stress. From Eq. (2), it is clear that pressure varies only in the axial direction. The constitutive equation of H-B fluid model is given by

$$-\frac{d\bar{u}}{d\bar{r}} = \begin{cases} \dfrac{1}{\bar{\eta}}\left(\bar{\tau}-\bar{\tau}_y\right)^n & \text{if} \quad \bar{\tau} > \bar{\tau}_y \\ 0 & \text{if} \quad \bar{\tau} \le \bar{\tau}_y \end{cases} \tag{3}$$

where $\bar{u}$ is the axial velocity of the fluid; η is the coefficient of viscosity of H-B fluid with dimension $\left(ML^{-1}T^{-2}\right)^n T$, n the is power-law index, $\bar{\tau}$ and $\bar{\tau}_y$ are the shear stress and yield stress, respectively. Eq. (3) implies that normal shear flow occurs in the region where the shear stress exceeds the yield stress and unshear flow (plug flow or solid-like flow) occurs in the region where the shear stress does not exceed the yield stress. Eqs. (1) and (2) can be solved for the unknowns shear stress $\bar{\tau}$ and velocity $\bar{u}$ with to the following boundary conditions.

$\bar{\tau}$ is finite at $\bar{r} = 0$ (4a)

$\bar{u} = 0$ at $\bar{r} = \bar{a}$ (4b)

For the unsteady dispersion of solutes in the steady flow of blood (represented by H-B fluid model), the simplified form of the species transport equation is given below.

$$\frac{\partial\bar{C}}{\partial\bar{t}} + \bar{u}\frac{\partial\bar{C}}{\partial\bar{z}} = \bar{D}_m\left(\bar{L}^2 + \frac{\partial^2}{\partial\bar{z}^2}\right)\bar{C} \tag{5}$$

where $\bar{L}^2 = (1/\bar{r})\partial/\partial\bar{r}\left(\bar{r}\left(\partial/\partial\bar{r}\right)\right)$, $\bar{C}(\bar{r},\bar{z},\bar{t})$ is the concentration of the solute, $\bar{t}$ is the time variable and $\bar{D}_m$ is the coefficient of molecular diffusivity. The initial and boundary conditions of the solute concentration $\bar{C}(\bar{r},\bar{z},\bar{t})$ are

$$\bar{C}(\bar{r},\bar{z},0) = \begin{cases} C_0, & \text{if } |\bar{z}| \le \dfrac{\bar{z}_s}{2} \\ 0, & \text{if } |\bar{z}| > \dfrac{\bar{z}_s}{2} \end{cases} \tag{6}$$

$$\bar{C}\left(\bar{r},\infty,\bar{t}\right)=0 \tag{7}$$

and

$$\frac{\partial\bar{C}}{\partial\bar{r}}\left(0,\bar{z},\bar{t}\right)=0=\frac{\partial\bar{C}}{\partial\bar{r}}\left(a,\bar{z},\bar{t}\right) \tag{8}$$

where $\bar{C}_0$ is the reference concentration.

2.1.2 Non-dimensional variables

Let us introduce the following non-dimensional variables.

$$C=\frac{\bar{C}}{\bar{C}_0},\ u=\frac{\bar{u}}{\bar{u}_0},\ r=\frac{\bar{r}}{\bar{a}},\ r_p=\frac{\bar{r}_p}{\bar{a}},\ z=\frac{\bar{D}_m\bar{z}}{\bar{a}^2\bar{u}_0},\ t=\frac{\bar{D}_m\bar{t}}{\bar{a}^2},\tau=\frac{\bar{\tau}}{\bar{a}\left(-d\bar{p}/d\bar{z}\right)},\tau_y=\frac{\bar{\tau}_y}{\bar{a}\left(-d\bar{p}/d\bar{z}\right)} \tag{9}$$

where

$$u_0=\frac{\bar{a}^{n+1}}{\left(n+1\right)\bar{\eta}}\left(-\frac{1}{2}\frac{d\bar{p}}{d\bar{z}}\right)^n \tag{10}$$

is the characteristic velocity. Integrating Eq. (1) with respect to $\bar{r}$ and then using the non-dimensional variables, trivially we get the expression for the shear stress in non-dimensional form as $\tau=2r$. From this shear stress expression, one can easily get the expression for the yield stress in non-dimensional form as $\tau_y=2r_p$. Using the non-dimensional variables in Eq. (3), we get the following non-dimensional form of the constitutive equation of H-B fluid model.

$$-\frac{du}{dr}=\begin{cases}\left(\tau-\tau_y\right)^n & \text{if } \tau>\tau_y\\ 0 & \text{if } \tau\le\tau_y\end{cases} \tag{11}$$

Non-dimensionalizing the boundary condition (4), we get

$$u=0 \text{ at } r=a \tag{12}$$

Applying the non-dimensional variables in Eq. (5), we obtain the non-dimensional form of the unsteady convective diffusion equation as below.

$$\frac{\partial C}{\partial t}+u\frac{\partial C}{\partial z}=\left(L^2+\frac{1}{Pe^2}\frac{\partial^2}{\partial z^2}\right)C \tag{13}$$

where

$$L^2=\frac{1}{r}\frac{\partial}{\partial r}\left(r\frac{\partial}{\partial r}\right) \tag{14}$$

and the Peclet number for the flow in pipe is defined as below [25]:

$$Pe=\frac{\bar{a}\,\bar{u}_0}{D_m}. \tag{15}$$

The non-dimensional form of the initial and boundary conditions for the concentration of the solute are

$$C(r,z,0)=\begin{cases}1, & \text{if } |z|\le \dfrac{z_s}{2}\\ 0, & \text{if } |z|>\dfrac{z_s}{2}\end{cases} \tag{17}$$

$$C(r,\infty,t)=0 \tag{18}$$

$$\frac{\partial C}{\partial r}(0,z,t)=0=\frac{\partial C}{\partial r}(1,z,t) \tag{19}$$

2.1.3 Solution method

Using two term binomial series approximation in Eq. (11) and then using Eq. (12), one can obtain the expression for the velocity of H-B fluid in the shear flow region as

$$u_+(r)=\left(1-r^{n+1}\right)-(n+1)r_p\left(1-r^n\right)+\frac{n(n+1)}{2}r_p^2\left(1-r^{n-1}\right) \quad \text{if} \quad r_p\le r\le 1 \tag{20}$$

The velocity of H-B fluid in the plug flow (unshear flow) region is obtained from Eq. (20) by evaluating it at $r=r_p$ and is given below:

$$u_-(r_p)=1-(n+1)r_p+\frac{n(n+1)}{2}r_p^2-\frac{n(n-1)}{2}r_p^{n+1} \qquad \text{if} \quad 0\le r\le r_p \tag{21}$$

where $r_p=\tau_y/2$. Using Eqs. (20) and (21), we get the expression for mean velocity as

$$u_m(r_p)=\frac{(n+1)}{(n+3)}\left[1-\frac{n(n+3)}{(n+2)}r_p+\frac{n(n+3)(n-1)}{2(n+1)}r_p^2-\frac{\left(n^4+2n^3-5n^2-6n+4\right)}{2(n+1)(n+2)}r_p^{n+3}\right] \tag{22}$$

Let us consider the convection of the solute across a plane which moves with the average velocity u_m of the fluid so that the axis moves with the mean speed of the fluid. For this moving coordinate, we define a new coordinate system (r, z_1, t) with the new axial coordinate z_1 which is defined as below.

$$z_1=z-u_m t \tag{23}$$

Using the generalized dispersion model of Gill and Sankarasubramanian [12], let us assume the solution of Eq. (18) in a series expansion involving $\partial^j C_m/\partial z_1^j$, as below.

$$C(r,z,t)=C_m(z,t)+\sum_{j=1}^{\infty}f_j(r,t)\frac{\partial^j C_m(z,t)}{\partial z_1^j} \tag{24}$$

where

$$C_m(z,t)=2\int_0^1 C(r,z,t)\,r\,dr \tag{25}$$

is the mean concentration of the solute over a cross section and f_j is the dispersion function associated with $\partial^j C_m/\partial z_1^j$. Substituting Eq. (24) in Eq. (13), one can obtain

$$\frac{\partial C_m}{\partial t}+(u-u_m)\frac{\partial C_m}{\partial z_1}-\frac{1}{Pe^2}\frac{\partial^2 C_m}{\partial z_1^2}+\sum_{j=1}^{\infty}\left[\left(\frac{\partial f_j}{\partial t}-L^2 f_j\right)\frac{\partial^j C_m}{\partial z_1^j}+(u-u_m)f_j\frac{\partial^{j+1}C_m}{\partial z_1^{j+1}}\right.$$

$$-\frac{1}{Pe^2} f_j \frac{\partial^{j+2} C_m}{\partial z_1^{j+2}} + f_j \frac{\partial^{j+1} C_m}{\partial t \, \partial z_1^{j}} \Bigg] = 0. \tag{26}$$

As pointed out by Dash et al. [26], we can assume that the process of distributing $C_m(z,t)$ is diffusive in nature right from the initial time and thus, one can write the generalized dispersion model for $C_m(z,t)$ as below with the dispersion coefficients $K_i(t)$ as suitable functions of time *t*.

$$\frac{\partial C_m}{\partial t} = \sum_{i=1}^{\infty} K_i(t) \frac{\partial^i C_m}{\partial z_1^i} \tag{27}$$

with the dispersion coefficients $K_1(t)$ as suitable functions of time *t*, where $K_1(t)$ is the coefficient of longitudinal convection and $K_2(t)$ is the coefficient of longitudinal diffusion. Since, the coefficient $K_2(t)$ expresses the whole dispersion process in terms of simple diffusion process; it is also called as the effective longitudinal diffusivity. Using Eq. (19) in Eq. (18) and grouping the coefficients of $\partial^j C_m / \partial z_1^j$, $j = 1, 2, \ldots$ together, one can obtain

$$\left[\frac{\partial f_1}{\partial t} - L^2 f_1 + (u - u_m) + K_1(t)\right] \frac{\partial C_m}{\partial z_1} + \left[\frac{\partial f_2}{\partial t} - L^2 f_2 + (u - u_m) f_1 + K_1(t) f_1 + K_2(t) - \frac{1}{Pe^2}\right] \frac{\partial^2 C_m}{\partial z_1^2}$$

$$+ \sum_{j=1}^{\infty} \left[\frac{\partial f_{j+2}}{\partial t} - L^2 f_{j+2} + (u - u_m) f_{j+1} - \frac{1}{Pe^2} f_j + \sum_{i=1}^{j+1} K_i(t) f_{j+2-i} + K_{j+2}(t)\right] \frac{\partial^{j+2} C_m}{\partial z_1^{j+2}} = 0 \tag{28}$$

In Eq.(20), equating the coefficients of $\partial^j C_m / \partial z_1^j$ to zero for $j = 1, 2, 3, \ldots$, we get the following infinite system of partial differential equations.

$$\frac{\partial f_1}{\partial t} - L^2 f_1 + (u - u_m) + K_1(t) = 0 \tag{29}$$

$$\frac{\partial f_2}{\partial t} - L^2 f_2 + \left[(u - u_m) + K_1(t)\right] f_1 + K_2(t) - \frac{1}{Pe^2} = 0 \tag{30}$$

$$\frac{\partial f_{j+2}}{\partial t} - L^2 f_{j+2} + \left[(u - u_m) + K_1(t)\right] f_{j+1} + \left[K_2(t) - \frac{1}{Pe^2}\right] f_j + \sum_{i=2}^{j+2} K_i(t) f_{j+2-i} = 0$$

for $j = 1, 2, \ldots,$ with $f_0 = 1.$ (31)

Since $C(r,z,t)$ is expressed in terms of $C_m(z,t)$ in Eq. (24), $C_m(z,t)$ can be chosen to satisfy the initial and boundary conditions of $C(r,z,t)$. The initial condition and boundary conditions for f_j can be obtained from Eqs. (17) – (19) and (24) and are given below.

$$f_j(r,0) = 0 \tag{32}$$

$$\frac{\partial f_j}{\partial r}(0,t) = 0 = \frac{\partial f_j}{\partial r}(1,t) \tag{33}$$

From Eqs. (24) and (25), one can obtain the solvability condition as given below.

$$\int_0^1 f_j \; r \; dr = 0. \tag{34}$$

Multiplying Eq. (29) by *r* and integrating between 0 and 1 and then making use of the solvability condition (34), one can get

$$K_1(t) = -2\int_0^1 (u - u_m) \; r \; dr = 0 \tag{35}$$

Similarly, applying the same procedure in Eqs. (30) and (31), we obtain

$$K_2(t) = \frac{1}{Pe^2} - 2\int_0^1 f_1 \, u \, r \, dr \tag{36}$$

$$K_{j+2}(t) = -2\int_0^1 f_{j+1} \; u \; r \; dr, \; j = 1, 2, \ldots \tag{37}$$

2.1.3.1 Solution of f_1

In Eq.(24), the function $f_1(r,t)$ known as dispersion function, is the coefficient of $\partial C_m / \partial z_1$ which plays a vital role in measuring the deviation of the local concentration $C(r,z,t)$ from the mean concentration $C_m(z,t)$. The solution of Eq. (29) satisfying the boundary conditions (32) and (33) can be expressed in the following form.

$$f_1(r,t) = f_{1s}(r) + f_{1t}(r,t) \tag{38}$$

where $f_{1s}(r)$ is the dispersion function in the steady state and $f_{1t}(r,t)$ is the dispersion function in the transient state which describes the time-dependent nature of the dispersion of the solute in the H-B fluid. Using Eq. (38) in Eq. (29), one can obtain the following equation.

$$\frac{\partial f_{1s}}{\partial t} + \frac{\partial f_{1t}}{\partial t} - L^2 f_{1s} - L^2 f_{1t} + (u - u_m) = 0 \tag{39}$$

Since, $\frac{\partial f_{1s}}{\partial t} = 0$ for steady flow, grouping the $f_{1t}(r,t)$ terms together and rest of the terms together and equating each of these to zero, we obtain the following simplified differential equations for the unknowns $f_{1s}(r)$ and $f_{1t}(r,t)$.

$$L^2 f_{1s} - (u - u_m) = 0 \tag{40}$$

$$\frac{\partial f_{1t}}{\partial t} = L^2 f_{1t} \tag{41}$$

Substituting Eq. (38) in Eqs. (32) and (33) and then applying the same procedure, we get the following simplified boundary conditions for $f_{1s}(r)$ and $f_{1t}(r,t)$.

$$f_{1t}(r,0) = -f_{1s}(r) \tag{42}$$

$$\frac{df_{1s}}{dr}(r=0) = 0 = \frac{df_{1s}}{dr}(r=1) \tag{43}$$

$$\frac{\partial f_{1t}}{\partial r}(0,t) = 0 = \frac{\partial f_{1t}}{\partial r}(1,t) \tag{44}$$

Similarly, using Eq. (38) in the solvability condition (34), one can obtain the following useful condition.

$$\int_0^1 f_{1t}\ r\ dr = -\int_0^1 f_{1s}\ r\ dr = 0 \tag{45}$$

Solving Eq. (40) subject to the condition (43), we get the steady state solution of the dispersion function $f_{1s}(r)$, where $f_{1s_-}(r)$ is defined in the plug core region and $f_{1s+}(r)$ is defined in the outer region, given by

$$f_{1s_-}(r) = \left[\frac{1}{2(n+3)} - \frac{(n+1)}{2(n+2)} r_p + \frac{n}{4} r_p^2 - \frac{n(n-1)}{8} r_p^{n+1} + \frac{\left(n^4+2n^3-5n^2-6n+4\right)}{8(n+2)(n+3)} r_p^{n+3}\right] r^2 + CI_1 \tag{46}$$

$$f_{1s_+}(r) = -\frac{\left(n^7+10n^6+32n^5+18n^4-93n^3-164n^2-52n+40\right)}{8(n+1)(n+2)^2(n+3)^2} r_p^{n+3}$$
$$+\left[\frac{1}{2(n+3)} - \frac{(n+1)}{2(n+2)} r_p + \frac{n}{4} r_p^2 + \frac{\left(n^4+2n^3-5n^2-6n+4\right)}{8(n+2)(n+3)} r_p^{n+3}\right] r^2$$
$$-\frac{\left(n^4+2n^3-5n^2-6n+4\right)}{4(n+2)(n+3)} r_p^{n+3} log\left(\frac{r}{r_p}\right) + \frac{(n+1)}{(n+2)^2} r_p r^{n+2} - \frac{n}{2(n+1)} r_p^2 r^{n+1} - \frac{1}{(n+3)^2} r^{n+3} + CI_1 \tag{47}$$

where

$$CI_1 = -\frac{(n+1)(n+7)}{4(n+3)^2(n+5)} + \frac{n(n+1)(n+6)}{4(n+2)^2(n+4)} r_p + \frac{n(n-1)(n+5)}{8(n+1)(n+3)} r_p^2$$
$$-\frac{\left(n^7+4n^6-10n^5-60n^4-39n^3+112n^2+128n-8\right)}{16(n+1)(n+2)^2(n+3)^2} r_p^{n+3}$$
$$+\frac{(n+1)\left(n^4+6n^3-3n^2-36n+24\right)}{1\ (n+6)(n+4)(n+5)} r_p^{n+5} - \frac{\left(n^4+2n^3-5n^2-6n+4\right)}{4(n+2)(n+3)} r_p^{n+3} log\left(r_p\right) \tag{48}$$

Solving Eq. (41) by the variable separable method subject to the boundary conditions (42), (44) – (45), we get the most general solution of $f_{1t}(r, t)$ as

$$f_{1t}(r,t) = \sum_{m=1}^{\infty} \left\{ A_m \lambda e^{-\lambda_m^2 t}\ J_0(\ _m r) \right\} \tag{49}$$

where

$$A_m = -\frac{\int_0^1 J_0(\lambda_m r) f_{1s}(r)\ r\ dr}{\int_0^1 \left[J_0(\lambda_m r)\right]^2 r\ dr} = -\frac{2}{J_0^2(\lambda_m)}\left[I_1 + I_2\right] \tag{50}$$

where

$$I_1 = \int_0^{r_p} J_0(\lambda_m r) f_{1s_-}(r) r\ dr \tag{51}$$

and

$$I_2 = \int_{r_p}^1 J_0(\lambda_m r) f_{1s_+}(r)\ r\ dr \tag{52}$$

where $J_0(\lambda_m r)$ and $J_1(\lambda_m r)$ denote the Bessel's functions of the first kind of order zero and one, respectively, and the eigen values λ_m's are the root of the equation $J_1(r)=0$. Evaluating the integrals in Eqs. (51) and (52), we get the expressions for B_1 and B_2, and these expressions are given in Appendix A.

2.1.3.2 Solution of diffusion coefficient $K_2(t)$

It is to be noted that $K_2(t)$ is a very useful dispersion coefficient appearing in the generalized dispersion model represented by Eq. (36) and is used to measure the dispersion of solute in the solvent (H-B fluid). Using Eqs. (20), (21), (38),(46) – (48), (50) – (52) in Eq. (36), we get the expression for the dispersion coefficient $K_2(t)$ and is given Appendix B. When the power-law index $n=1$, and yield stress $\tau_y=0$, the H-B fluid model reduces to Newtonian fluid model and in this case, the present model reduces to the Taylor-Aris dispersion model of Newtonian fluid. Applying the aforementioned values of the power-law index and yield stress in Eqs. (36) and (37), we get the values of the coefficient of longitudinal convection $K_1(t)$ and coefficient of longitudinal diffusion $K_2(t)$ for the dispersion of solute in Newtonian fluid flow as zero and $(1/Pe^2)+(1/192)$ respectively. So, if the higher order terms in Eq. (27) are neglected, then it reduces to a simple diffusion equation for $C_m(z,t)$ with diffusion coefficient as $K_2(t)$. Once $K_2(t)$ is known, $f_2(r,t)$ can be obtained from Eq. (30). The method of obtaining $f_2(r,t)$ from Eq. (30) is very similar to the method that was applied to get $f_1(r,t)$. Substitution of the expression of $f_2(r,t)$ in Eq. (37) yields $K_3(t)$ and proceeding in a similar way, one can find $f_3(r,t)$, $K_4(t)$, $f_4(r,t)$, $K_5(t)$ and so on from Eqs. (31) and (37) recursively. Since the solutions obtained for $f_1(r,t)$ and $K_2(t)$ are very lengthy and highly complicated, it is cumbersome to find the higher order dispersion function $f_2(r,t)$ and diffusion coefficient $K_3(t)$ and so on.

Since the value of the dispersion coefficient $K_3(t)$ for Newtonian fluid is $K_3(t\to\infty)=-1/23040$ which is negligibly small, the magnitude of the higher order coefficients decreases very significantly [26]. It is also observed that the dispersion coefficients $K_{j+2}(j=1,2,...)$ can be calculated from Eq. (37), but the values of these dispersion coefficients are very small when compared to $K_2(t)$ and hence, in the present study, we have ignored the computation of the dispersion coefficients $K_{j+2}(j=1,2,...)$.

2.1.3.3 Solution for mean concentration $C_m\left(z_1,t\right)$

Since the magnitude of the coefficients $K_3\left(t\right)$, $K_4\left(t\right), K_5\left(t\right),.....$ are negligibly small, on neglecting the terms involving these coefficients, Eq. (27) simplifies to

$$\frac{\partial C_m}{\partial t} = K_2\left(t\right)\frac{\partial^2 C_m}{\partial z_1^2}. \tag{53}$$

The mean concentration of the solute $C_m\left(z_1,t\right)$ has the following initial and boundary conditions.

$$C_m\left(z_1,0\right) = \begin{cases} 1 & \text{if } \left|z_1\right| \le z_s/2 \\ 0 & \text{if } \left|z_1\right| \ge z_s/2 \end{cases} \tag{54}$$

$$C_m\left(\infty,t\right) = 0 \tag{55}$$

Solving Eq. (53) subject to the initial and boundary conditions (54) and (55), we obtain the expression for mean concentration of the solute as [25]

$$C_m\left(z,t\right) = \frac{1}{2}\left[erf\left(\frac{\left(z_s/2\right)-z_1}{2\xi^{1/2}}\right) + erf\left(\frac{\left(z_s/2\right)+z_1}{2\xi^{1/2}}\right)\right] \tag{56}$$

where

$$\xi\left(t\right) = \int_0^t K_2\left(t\right)\,dt \tag{57}$$

From Eq.(56), one can observe that at any time *t*, the mean concentration $C_m\left(z_1,t\right)$ is symmetric about a point which moves with the average velocity $u_m\left(r_p\right)$ of the fluid. Substituting the expressions obtained so far for the mean concentration $C_m\left(z_1,t\right)$ and the dispersion function $f_1\left(r,t\right)$ in Eq. (24) (neglecting the higher order terms), one can get the expression for the local concentration $C\left(r,z_1,t\right)$ (with first order approximation) as given below.

$$C\left(r,z_1,t\right) = C_m\left(z_1,t\right) + f_1\left(r,t\right)\frac{\partial C_m}{\partial z_1}\left(z_1,t\right) \tag{58}$$

2.2 Flow in Channel

2.2.1 Governing equations

Consider the unsteady dispersion of a bolus of solute of initial length $\overline{z}_s$ units in the steady, laminar and fully developed slow flow of viscous incompressible non-Newtonian fluid through a channel of width $2\overline{h}$ bounded by two parallel flat plates. We consider the non-Newtonian fluid flowing in the channel as Herschel-Bulkley (H-B) fluid model. Cartesian coordinate system $\left(\overline{x},\overline{z}\right)$ is used to analyze the flow between the parallel flat plates, where $\overline{x}$ and $\overline{z}$ are the coordinates taken in the vertical (transverse) and axial (longitudinal) directions respectively, as shown in Fig. 1(b). For the steady flow of viscous incompressible (H-B) fluid, the momentum

equations in the axial and transverse directions reduce to the following equations.

$$\frac{d\bar{p}}{d\bar{z}} = -\frac{d}{d\bar{x}}(\bar{\tau}) \tag{59}$$

and

$$\frac{d\bar{p}}{d\bar{x}} = 0 \tag{60}$$

where $\bar{p}$ is the pressure and $\bar{\tau}$ is the shear stress. Eq. (60) implies that pressure is constant in the transverse direction $\bar{x}$ and it varies only in the axial direction $\bar{z}$. The constitutive equation of the H-B fluid is given by

$$-\frac{d\bar{u}}{d\bar{x}} = \begin{cases} \frac{1}{\eta}\left(\bar{\tau} - \bar{\tau}_y\right)^n & \text{if} \quad \bar{\tau} > \bar{\tau}_y \\ 0 & \text{if} \quad \bar{\tau} \le \bar{\tau}_y \end{cases} \tag{61}$$

where $\bar{u}$ is the velocity of the fluid in the axial direction, η is the coefficient of viscosity (at high rate of shear) of H-B fluid model with dimension $\left(ML^{-1}T^{-2}\right)^n T$, n the is power-law index, $\bar{\tau}_y$ is the yield stress. Eqs. (59) and (61) form the system of nonlinear differential equations which can be solved for the unknowns shear stress $\bar{\tau}$ and velocity $\bar{u}$ with the following boundary conditions.

$$\bar{\tau} \text{ is finite at } \bar{x} = 0 \tag{62}$$

$$\bar{u} = 0 \text{ at } \bar{x} = \bar{h} \tag{63}$$

The simplified form of the unsteady convective diffusion equation for the dispersion of solute in the steady, laminar, fully developed flow of H-B fluid is given below.

$$\frac{\partial \bar{C}}{\partial \bar{t}} + \bar{u}\frac{\partial \bar{C}}{\partial \bar{z}} = \bar{D}_m\left(\bar{L}^2 + \frac{\partial^2}{\partial \bar{z}^2}\right)\bar{C} \tag{64}$$

where $\bar{L} = \partial/\partial\bar{x}$, $\bar{C}$ is the concentration of the solute, $\bar{t}$ is the time of the dispersion process and $\bar{D}_m$ is the coefficient of molecular diffusion. The initial and boundary conditions governing the flow are

$$\bar{C}\left(\bar{x}, \bar{z}, \bar{t}\right) = \begin{cases} C_0, & \text{if } \left|\bar{z}\right| \le \frac{\bar{z}_s}{2} \\ 0, & \text{if } \left|\bar{z}\right| > \frac{\bar{z}_s}{2} \end{cases} \tag{65}$$

$$\bar{C}\left(\bar{x}, \infty\, \bar{t}\right) = 0 \tag{66}$$

$$\frac{\partial \bar{C}}{\partial \bar{x}}\left(0, \bar{z}\ \bar{t}\right) = 0 = \frac{\partial \bar{C}}{\partial \bar{x}}\left(\bar{h}, \bar{z}\ \bar{t}\right) \tag{67}$$

2.2.2 Non-dimensional variables

Let us introduce the following non-dimensional variables.

$$C = \frac{\bar{C}}{\bar{C}_0},\ u = \frac{\bar{u}}{\bar{u}_0},\ x = \frac{\bar{x}}{\bar{h}},\ x_p = \frac{\bar{x}_p}{\bar{h}},\ z = \frac{\bar{D}_m \bar{z}}{\bar{h}^2 \bar{u}_0},\ t = \frac{\bar{D}_m \bar{t}}{\bar{h}^2},\ \tau = \frac{\bar{\tau}}{\bar{h}\left(-d\bar{p}/d\bar{z}\right)},\ \tau_y = \frac{\bar{\tau}_y}{\bar{h}\left(-d\bar{p}/d\bar{z}\right)} \tag{68}$$

where

$$u_0 = \frac{h^{n+1}}{(n+1)\eta}\left(-\frac{1}{2}\frac{d\bar{p}}{d\bar{z}}\right)^n \tag{69}$$

is the characteristic velocity. Integrating Eq. (59) with respect to $\bar{x}$ and then using the non-dimensional variables (68), we get the expression for the shear stress as $\tau = x$. Replacing x by x_p in $\tau = x$, one can easily obtain the expression for yield stress as $\tau_y = x_p$.

Applying the non-dimensional variables (68) in Eq. (61), we obtain the non-dimensional form of the constitutive equation of H-B fluid model as below.

$$-\frac{du}{dx} = \begin{cases} (\tau - \tau_y)^n & \text{if} \quad \tau > \tau_y \\ 0 & \text{if} \quad \tau \le \tau_y \end{cases} \tag{70}$$

The non-dimensional form of the boundary condition (63) is

$$u = 0 \text{ at } x = h \tag{71}$$

Substituting the non-dimensional variables (68) into Eq. (64) one can get the non-dimensional form of the unsteady convective diffusion as given below.

$$\frac{\partial C}{\partial t} + u\frac{\partial C}{\partial z} = \left(L^2 + \frac{1}{Pe^2}\frac{\partial^2}{\partial z^2}\right)C \tag{72}$$

where $L = \partial/\partial x$ and $Pe = \bar{h}\bar{u}_0/\bar{D}_m$ is the Peclet number. The non-dimensional form of the initial and boundary conditions (65)-(67) for the concentration $C(z,x,t)$ of the solute are

$$C(x,\, z,\, 0) = \begin{cases} 1 & \text{if} \quad |z| \le z_s/2 \\ 0 & \text{if} \quad |z| > z_s/2 \end{cases} \tag{73}$$

$$C(x,\, \infty,\, t) = 0 \tag{74}$$

$$\frac{\partial C}{\partial x}(0,\, z,\, t) = 0 = \frac{\partial C}{\partial x}(1,\, z,\, t) \tag{75}$$

2.2.3 Method of solution

Applying binomial series expansion for $(\tau - \tau_y)^n$ in Eq. (70) and then approximating the series expansion to first two terms followed by, making use of $\tau = x$, $\tau_y = x_p$ and Eq. (71) in the resulting equation. Hence, we obtain the expression for the velocity of the H-B fluid in the outer flow (shear flow) region in the form

$$u_+(x) = 1 - x^{n+1} - (n+1)x_p(1 - x^n) + \frac{n(n+1)}{2}x_p^2(1 - x^{n-1}) \tag{76}$$

The velocity of the H-B fluid in the plug flow (unshear flow) region is obtained from Eq. (76) by replacing x by x_p and is given below.

$$u_{-}\left(x_p\right)=1-\left(n+1\right)x_p+\frac{n\left(n+1\right)}{2}x_p^2-\frac{n\left(n-1\right)}{2}x_p^{n+1} \tag{77}$$

Using Eqs. (76) and (77), we get the expression for the mean velocity as below.

$$u_m\left(x_p\right)=\frac{\left(n+1\right)}{\left(n+2\right)}\left[1-\frac{n\left(n+2\right)}{\left(n+1\right)}x_p+\frac{\left(n-1\right)\left(n+2\right)}{2}x_p^2-\frac{n\left(n^2-3\right)}{2\left(n+1\right)}x_p^{n+2}\right] \tag{78}$$

Let the solute's convection occurs across a plane which moves with the average velocity u_m of the H-B fluid so that the axis is moving with the mean speed of the H-B fluid flow. Hence, we define a new coordinate system $\left(x,\, z_1\right)$ with the new axial coordinate z_1 defined by

$$z_1=z-u_m\ t \tag{79}$$

Using the generalized dispersion model of Gill and Sankarasubramanian [12], let us assume the solution of Eq. (72) as a derivative series expansion involving $\partial^j C_m/\partial z_1^j$, as given below.

$$C\left(x,z_1,t\right)=C_m\left(z_1,t\right)+\sum_{j=1}^{\infty}f_j\left(x,t\right)\frac{\partial^j C_m}{\partial z_1^j}\left(z_1,t\right) \tag{80}$$

where

$$C_m\left(z_1,\,t\right)=\int_0^1 C\left(x,\,z_1\ t\right)\,dx \tag{81}$$

is the mean concentration of the solute over a cross section, $f_j\left(x,\,t\right)$ dispersion function corresponding to $\partial^j C_m/\partial z_1^j$. Using Eq. (80) in Eq. (72), one can get

$$\frac{\partial C_m}{\partial t}+\left(u-u_m\right)\frac{\partial C_m}{\partial z_1}-\frac{1}{Pe^2}\frac{\partial^2 C_m}{\partial z_1^2}+\sum_{j=1}^{\infty}\left[\left(\frac{\partial f_j}{\partial t}-L^2 f_j\right)\frac{\partial^j C_m}{\partial z_1^j}+\left(u-u_m\right)f_j\frac{\partial^{j+1}C_m}{\partial z_1^{j+1}}\right.$$

$$\left.\frac{1}{Pe^2}f_j\frac{\partial^{j+2}C_m}{\partial z_1^{j+2}}+f_j\frac{\partial^{j+1}C_m}{\partial t\partial z_1^j}\right]=0 \tag{82}$$

As in the section 2.1.3, let us express the generalized dispersion model for $C_m\left(z_1,\,t\right)$ with the dispersion coefficients $K_i\left(t\right)$ as function of time t is shown as below.

$$\frac{\partial C_m}{\partial t}=\sum_{i=1}^{\infty}K_i\left(t\right)\frac{\partial^i C_m}{\partial z_1^i} \tag{83}$$

The physical significance of $K_1\left(t\right)$ and $K_2\left(t\right)$ in the dispersion of solutes is mentioned in section 2.1.3. Using Eq. (83) in Eq. (82) and grouping the coefficients of $\partial^j C_m/\partial z_1^j$, $j=1,2,....$ together, one can obtain

$$\left[\frac{\partial f_1}{\partial t}-L^2 f_1+\left(u-u_m\right)+K_1\left(t\right)\right]\frac{\partial C_m}{\partial z_1}+\left[\frac{\partial f_2}{\partial t}-L^2 f_2+\left(u-u_m\right)f_1+K_1\left(t\right)f_1+K_2\left(t\right)-\frac{1}{Pe^2}\right]\frac{\partial^2 C_m}{\partial z_1^2}$$

$$+\sum_{j=1}^{\infty}\left[\frac{\partial f_{j+2}}{\partial t}-L^2 f_{j+2}+\left(u-u_m\right)f_{j+1}-\frac{1}{Pe^2}f_j+\sum_{i=1}^{j+1}K_i\left(t\right)f_{j+2-i}+K_{j+2}\left(t\right)\right]\frac{\partial^{j+2}C_m}{\partial z_1^{j+2}}=0 \qquad (84)$$

As in section 2.1.3, equating the coefficients of $\partial^j C_m/\partial z_1^j$ to zero in the above equation for $j=1,2,3,\ldots$, we obtain the following infinite system of partial differential equations.

$$\frac{\partial f_1}{\partial t}-L^2 f_1+\left(u-u_m\right)+K_1\left(t\right)=0 \qquad (85)$$

$$\frac{\partial f_2}{\partial t}-L^2 f_2+\left[\left(u-u_m\right)+K_1\left(t\right)\right]f_1+K_2\left(t\right)-\frac{1}{Pe^2}=0 \qquad (86)$$

$$\frac{\partial f_{j+2}}{\partial t}-L^2 f_{j+2}+\left[\left(u-u_m\right)+K_1\left(t\right)\right]f_{j+1}+\left[K_2\left(t\right)-\frac{1}{Pe^2}\right]f_j+\sum_{i=2}^{j+2}K_i\left(t\right)f_{j+2-i}=0$$

for $j=1,2,\ldots,$ with $f_0=1.$ (87)

Since $C\left(x,z_1,t\right)$ is expressed in terms of $C_m\left(z_1,t\right)$ in Eq. (80), $C_m\left(z_1,t\right)$ can be chosen to satisfy the initial and boundary conditions of $C\left(x,z_1,t\right)$. The initial and boundary conditions for $f_j\left(x,t\right)$ can be obtained from (73)-(75) and (80) as below.

$$f_j\left(x,0\right)=0 \qquad (88)$$

$$\frac{\partial f_j}{\partial x}\left(0,t\right)=0=\frac{\partial f_j}{\partial x}\left(1,t\right) \qquad (89)$$

From Eqs. (80) and (81) we get the solvability condition as

$$\int_0^1 f_j\left(x,t\right)dx=0 \qquad (90)$$

Integrating Eq. (85) with respect to x from 0 to 1 and then using the solvability condition (90), one can get

$$K_1\left(t\right)=-\int_0^1\left(u-u_m\right)dx=0 \qquad (91)$$

Applying the similar procedure to Eqs. (86) and (87), we get

$$K_2\left(t\right)=\frac{1}{Pe^2}-\int_0^1 f_1\,u\,dx \qquad (92)$$

$$K_{j+2}\left(t\right)=-\int_0^1 f_{j+1}\,u\,dx,\ j=1,2,\ldots \qquad (93)$$

2.2.3.1 Solution of $f_1\left(x,t\right)$ and $K_2\left(t\right)$

As in the subsection 2.1.3.1, let us express $f_1\left(x,t\right)$ as below.

$$f_1\left(x,t\right)=f_{1s}\left(x\right)+f_{1t}\left(x,t\right) \qquad (94)$$

where $f_{1s}\left(x\right)$ is the steady part of the dispersion function and $f_{1t}\left(x,t\right)$ is the unsteady part of the dispersion function. Using Eq. (94) in Eq. (85) and proceeding in the same way as in subsection 2.1.3.1, we get the following differential equations respectively

for $f_{1s}(x)$ and $f_{1t}(x,t)$.

$$L^2 f_{1s} - (u - u_m) = 0 \tag{95}$$

$$\frac{\partial f_{1t}}{\partial t} = L^2 f_{1t} \tag{96}$$

As in the subsection 2.1.3.1, one can obtain the boundary and initial conditions of $f_{1s}(x)$ and $f_{1t}(x,t)$ as below.

$$\frac{df_{1s}}{dx}(x=0) = 0 = \frac{df_{1s}}{dx}(x=1) \tag{97}$$

$$\frac{\partial f_{1t}}{\partial x}(0,t) = 0 = \frac{\partial f_{1t}}{\partial x}(1,t). \tag{98}$$

$$f_{1t}(x,0) = -f_{1s}(x) \tag{99}$$

The solvability condition (90) takes the following form.

$$\int_0^1 f_{1t}\, dx = -\int_0^1 f_{1s}\, dx \tag{100}$$

Solving Eq. (95) subject to the boundary conditions (97), we get the following expressions for steady state dispersion function in the plug core and non-plug core regions, respectively.

$$f_{1s_-}(x) = \left[\frac{1}{2(n+2)} - \frac{1}{2}x_p + \frac{(n+1)}{4}x_p^2 - \frac{n(n-1)}{4}x_p^{n+1} + \frac{n(n^2-3)}{4(n+2)}x_p^{n+2}\right]x^2 - CI_2 \tag{101}$$

$$\begin{aligned} f_{1s_+}(x) &= \frac{(n^4+2n^3-5n^2-6n+4)}{4(n+2)(n+3)}x_p^{n+3} - \frac{n(n^2-3)}{2(n+2)}x_p^{n+2}x \\ &+ \left[\frac{1}{2(n+2)} - \frac{1}{2}x_p + \frac{(n+1)}{4}x_p^2 + \frac{n(n^2-3)}{4(n+2)}x_p^{n+2}\right]x^2 \\ &- \frac{1}{2}x_p x^{n+1} + \frac{1}{(n+2)}x_p x^{n+2} - \frac{1}{(n+2)(n+3)}x^{n+3} - CI_2 \end{aligned} \tag{102}$$

where

$$\begin{aligned} CI_2 &= -\frac{(n-3)}{6(n+2)(n+3)} + \frac{n(n+5)}{6(n+2)(n+3)}x_p + \frac{(n-1)(n+4)}{1\ \ (n+22)}x_p^2 - \frac{n(n^2-3)}{6(n+2)}x_p^{n+2} \\ &- \frac{(n^4-2n^3-5n^2-6n-4)}{4(n+2)(n+3)}x_p^{n+3} + \frac{(n+1)(n^4+4n^3-5n^2-18n+12)}{1\ \ (n+22)(n+3)(n+4)}x_p^{n+4} \end{aligned} \tag{103}$$

Solving Eq. (96) by variables separable method, we get the solution for $f_{1t}(x,t)$ and is given below [26].

$$f_{1t}(x,t) = \sum_{m=1}^{\infty}\left\{A_m\, e^{-\lambda_m^2 t}\, cos(\lambda_m x)\right\} \tag{104}$$

where

$$A_n = -\frac{\int_0^1 cos\left(\lambda_n x\right) f_{1s}\left(x\right) dx}{\int_0^1 cos^2\left(\lambda_n x\right) dx} = -2\int_0^1 cos\left(\lambda_n x\right) f_{1s}\left(x\right) dx = -2\left[I_3 + I_4\right] \tag{105}$$

where

$$I_3 = \int_0^{rp} cos\left(\lambda_n x\right) f_{1s_-}\left(x\right) dx = \left[\frac{1}{2\left(n+2\right)} - \frac{1}{2}x_p + \frac{\left(n+1\right)}{4}x_p^2 - \frac{n\left(n-1\right)}{4}x_p^{n+1} + \frac{n\left(n^2-3\right)}{4\left(n+2\right)}x_p^{n+2}\right]$$

$$\times\left[\frac{\left(x_p^2\lambda_n^2 - 2\right)sin\left(x_p\lambda_n\right)}{\lambda_n^3} + \frac{2x_p\, cos\left(x_p\lambda_n\right)}{\lambda_n^2}\right] - \frac{sin\left(x_p\lambda_n\right)}{\lambda_n}CI \tag{106}$$

and $I_4 = \int_{rp}^1 cos\left(\lambda_n x\right) f_{1s_+}\left(x\right) dx.$ This expression is evaluated using *Mathematica* and data required from this part for plotting the graphs is obtained directly from *Mathematica*. Using Eqs. (94), (101)-(106) in Eq. (92), we get the expression for $K_2\left(t\right)$ and is given in Appendix C. Since the solution of mean concentration $C_m\left(z_1,t\right)$ is the same as in the case of flow in pipe in subsection 2.1.3.3 (Eqs. (53)-(57)), we have not repeated the same procedure here. The expression for the concentration of the solution in the flow through channel is given below.

$$C\left(x,z_1,t\right) = C_m\left(z_1,t\right) + f_1\left(x,t\right)\frac{\partial C_m}{\partial z_1}\left(z_1,t\right) \tag{107}$$

3. Results and discussion

The main objective of the present study is to analyze mathematically the unsteady dispersion of a solute in H-B fluid flowing through (i) pipe and (ii) channel between parallel flat plates and provide some possible applications of this study to blood flow in narrow arteries when a bolus of solute is injected into the blood stream. It is also aimed to discuss the effects of the physical parameters such as yield stress, power-law index and time on the physiologically important flow quantities such as longitudinal dispersion coefficient relative effective diffusivity and relative axial diffusivity.

3.1 Longitudinal dispersion

In the investigation of the shear augmented dispersion of solutes in blood (modeled as H-B fluid) flow, the coefficient of effective longitudinal diffusion $K_2\left(t\right)$ is a physiologically important measurement which describes the entire dispersion process in terms of a simple diffusion process in the axial direction z_1. Figs. 2(a) and 2(b) sketch the variation of the dispersion coefficient $192\left[K_2\left(t\right) - \left(1/Pe^2\right)\right]$ with time in the dispersion of solutes in pipe flow and the dispersion coefficient

$(945/8)\left[K_2(t)-\left(1/Pe^2\right)\right]$ with time in channel flow, respectively, for different values of the plug core radius with n = 0.95. It is noted that the dispersion coefficient (effective longitudinal diffusion) increases rapidly (nonlinearly) with the increase of time t from 0 to 0.1 and then it increases slowly with the increase of time t from 0.1 to 0.2. Then, it becomes almost constant with the increase of time t from 0.2 to 0.5. It means that the solute diffuses rapidly in the solvent in the beginning of the dispersion process and then it diffuses very slowly or constantly after some time (when time t takes large values). It is also observed that dispersion process is relatively faster in pipe flow when compared with that in channel flow. It is also seen that the dispersion coefficient (longitudinal diffusion coefficient) decreases considerably with the increase of the plug core radius both in the cases of solutes dispersion in pipe flow and channel flow. Since the yield stress of the flowing fluid is equal to the radius/semi width of the plug flow region, one can note that the increase in the yield stress value of H-B fluid considerably reduces the longitudinal diffusion of solutes in both pipe and channel flow.

The variations of dispersion coefficient $192\left[K_2(t)-\left(1/Pe^2\right)\right]$ with time in pipe flow and the dispersion coefficient $(945/8)\left[K_2(t)-\left(1/Pe^2\right)\right]$ with time in channel flow for different fluid models are depicted in Figs. 3(a) and 3(b), respectively. It is noticed that the dispersion coefficient (longitudinal diffusion of solutes in Newtonian fluid flow is higher than that in power-law fluid flow and also higher than that in H-B/Bingham/Casson fluid flow. It is also found that the solutes dispersion in H-B fluid flow is significantly higher than that in Casson fluid flow. One can easily note that the solute dispersion reduces with the increase of the power-law index n of H-B fluid. It is of interest to note that the plots for the solutes dispersion in Newtonian fluid flow in both pipe and channel flow are in good agreement with the corresponding plots in Fig. 2(a) and 2(b) of Dash et al. [26]. The dispersion of solutes in any solvent fluid is found to be marginally higher in flow through pipe than that in flow through channel.

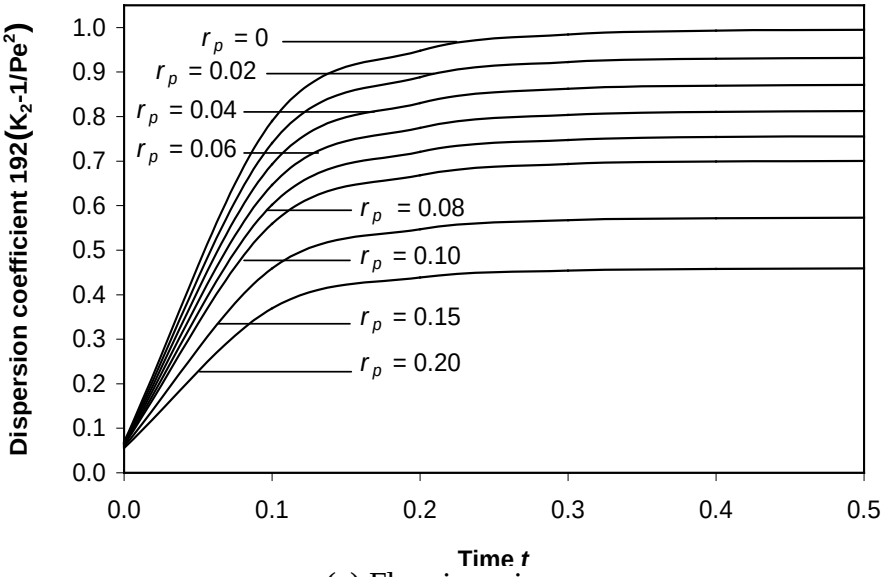

(a) Flow in a pipe.

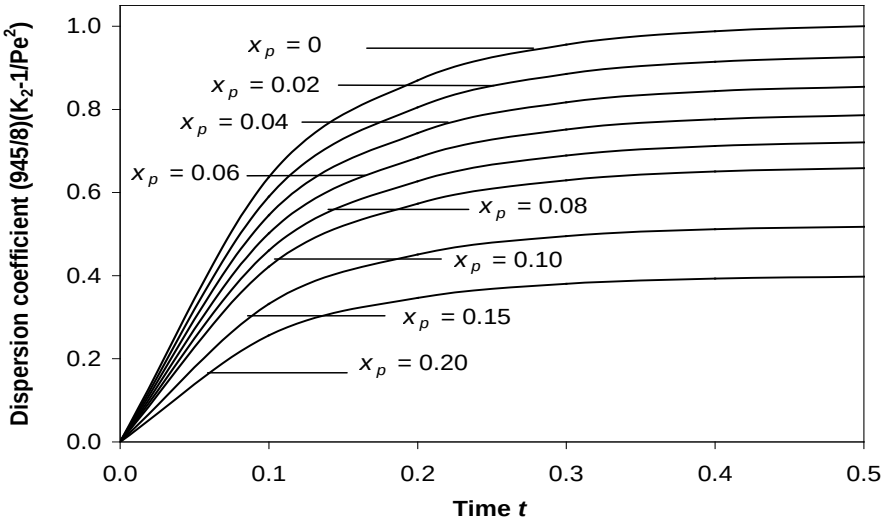

(b) Flow in a channel.

Figure 2: Variation of the dispersion coefficient with time t for different values of the radius/semi-width of the plug core region with $n = 0.95$ in (a) pipe and (b) channel.

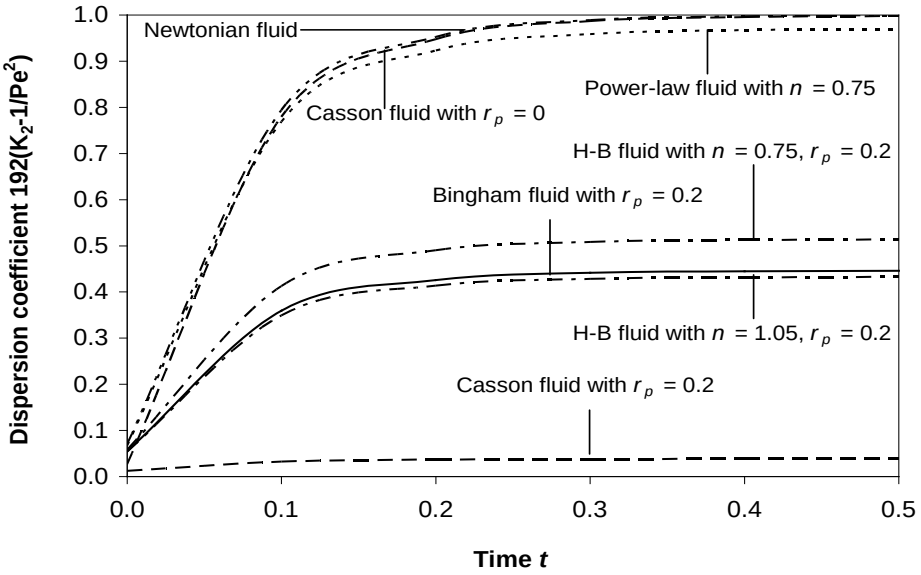

a. Flow in a pipe.

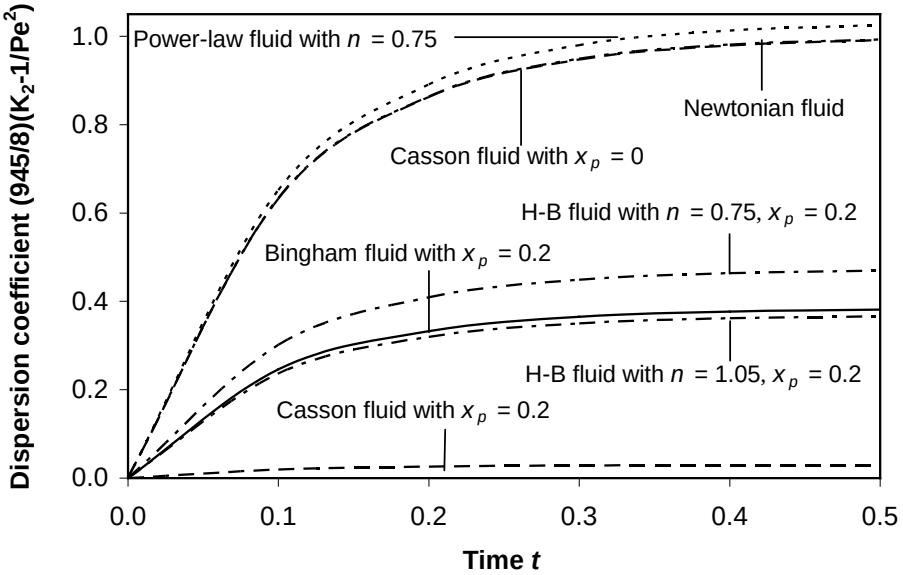

b. Flow in a channel.

Figure 3: Variation of dispersion coefficient with time for different fluid models in (a) pipe and (b) channel.

3.2 Relative axial diffusivity

The variation of relative axial diffusivity with time for different values of radius/semi-width of the plug core region with $n = 0.95$ for flow in pipe and channel are illustrated in Figs. 4(a) and 4(b). It is found that in both the cases of dispersion of solutes through pipe and channel, the relative effective diffusivity decreases very slowly initially and thereafter it is almost constant, i.e. soon after the initial time, it attains steady state. One can note that the relative axial diffusivity decreases considerably

with the increase of the radius/semi-width of the plug core region. It is noticed that the relative axial diffusivity is considerably higher in the flow through pipe when compared to the flow through channel. Figs. 5(a) and 5(b) sketches the variation of relative axial diffusivity with time for the dispersion of solutes in different fluid models flow through pipe and channel. It is observed that the relative effective diffusivity is significantly higher when the solutes disperse in H-B fluid flow than when the solutes disperse in Casson fluid flow. It is also clear that the effective diffusivity of the solutes decreases considerably with the increase of the power-law index of the H-B fluid.

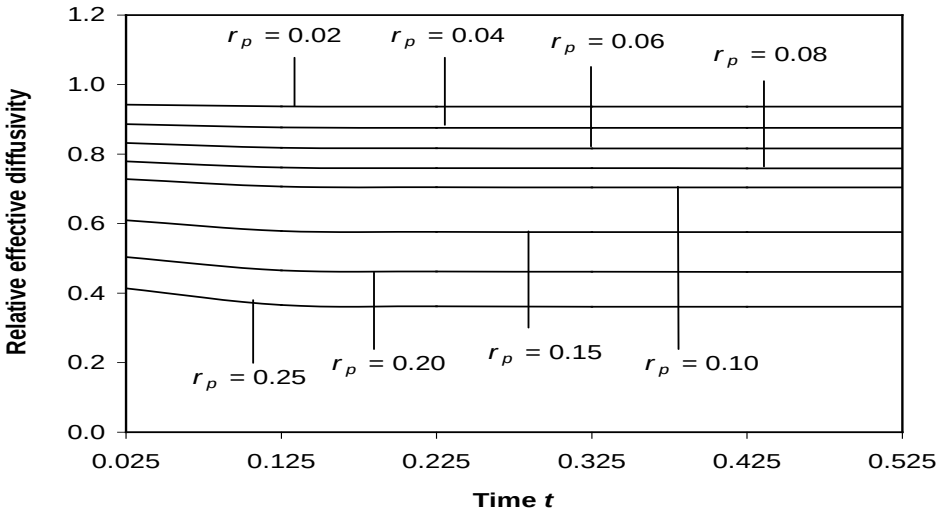

(a) Flow in a pipe.

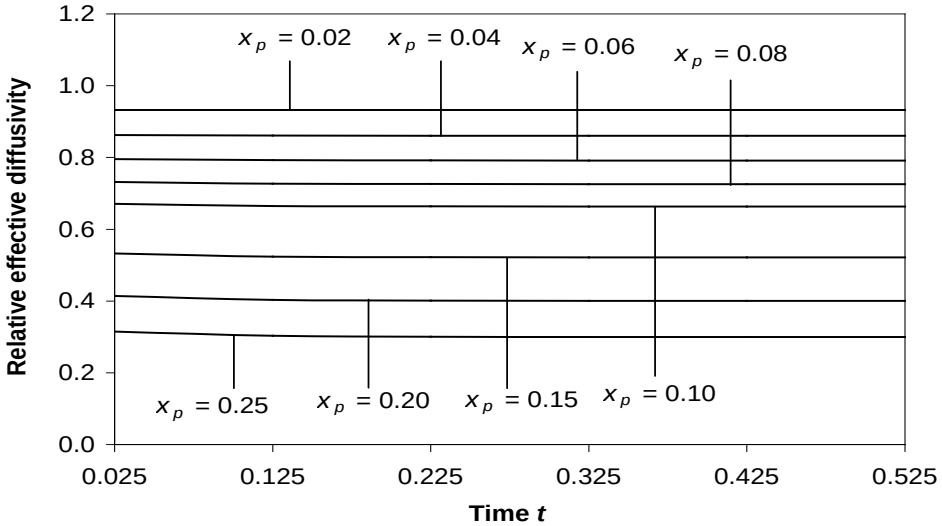

(b) Flow in a channel.

Figure 4: Variation of the relative effective diffusivity with time *t* for different values of the radius/semi-width of the plug flow region with n = 0.95 in (a) pipe and (b) channel.

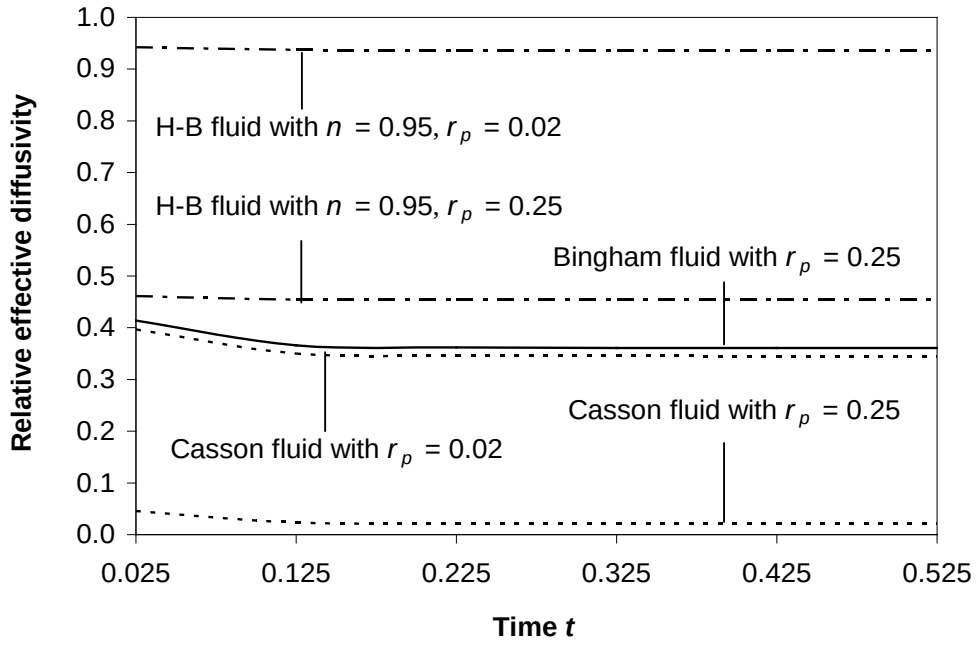

(a) Flow in a pipe.

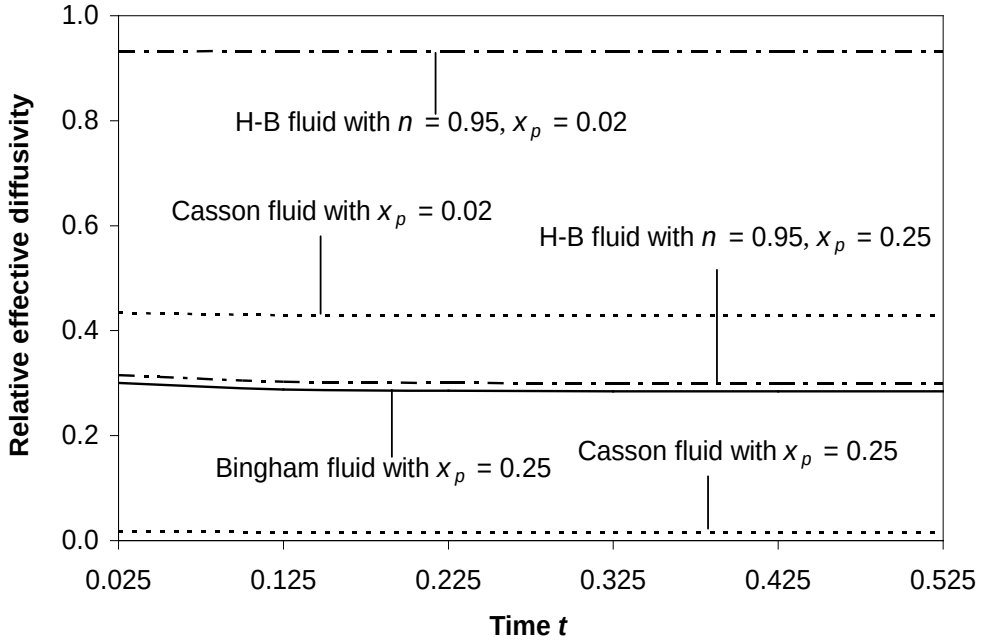

(b) Flow in a channel.

Figure 5: Variation of relative effective diffusivity with time for different fluid models in (a) pipe and (b) channel.

3.3 Distribution of dispersion function

The dispersion function f_1 measures the deviation of the concentration C of the

solutes from the mean concentration C_m of the solutes. The evolution of the dispersion function f_1 over time for dispersion of solutes in flow through pipe and channel for different values of the radius/semi-width of the plug core region with n = 0.95 are shown in Figs. 6 and 7 respectively. It is observed that for $r_p = x_p = 0$, the magnitude of the dispersion function f_1 is maximum, i.e. the solute dispersion is maximum in the absence of the plug core in the flow stream. It is also noted that the magnitude of the dispersion function f_1 increases with time, but it decreases with the increase of the radius$\left(r_p\right)$/semi-width$\left(x_p\right)$ of the plug core region. It is seen that for a given r_p or x_p, the plots of the dispersion function passes through a common point for all time. This is the point where the local concentration C of the solute is same as the mean concentration C_m of the solute.

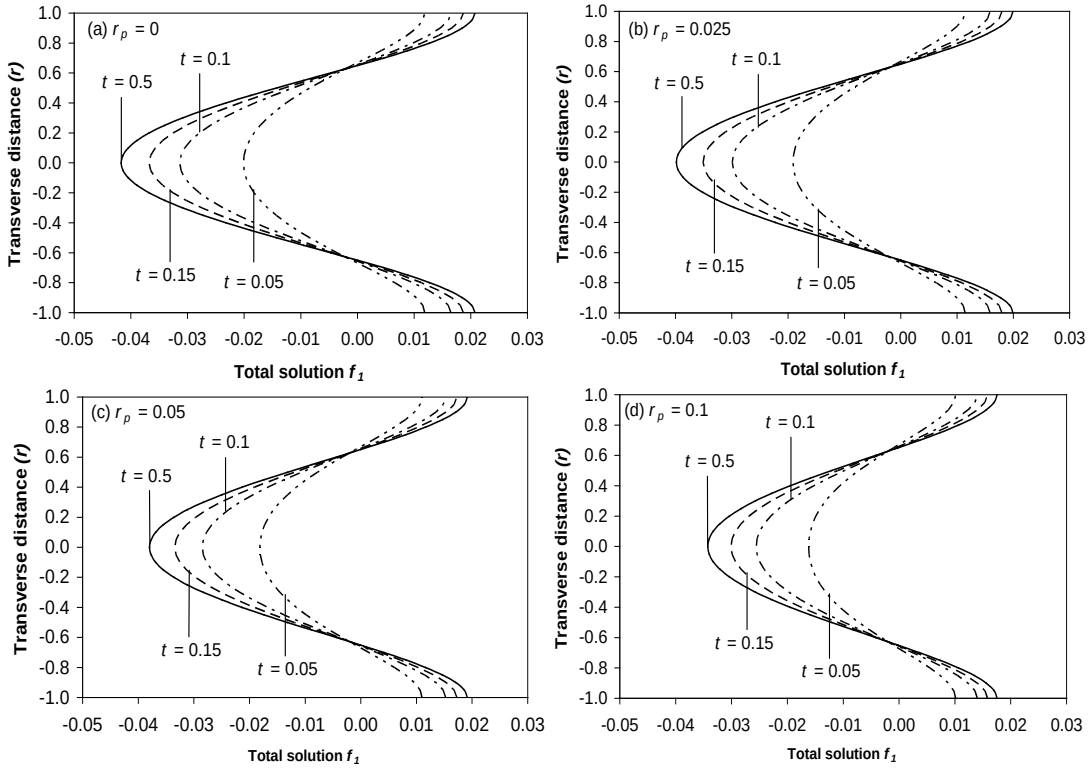

Figure 6: Distribution of total solution f_1 at different instants of time *t* for dispersion in a pipe with (a) $r_p = 0$, (b) $r_p = 0.025$, (c) $r_p = 0.05$ and (d) $r_p = 0.1$.

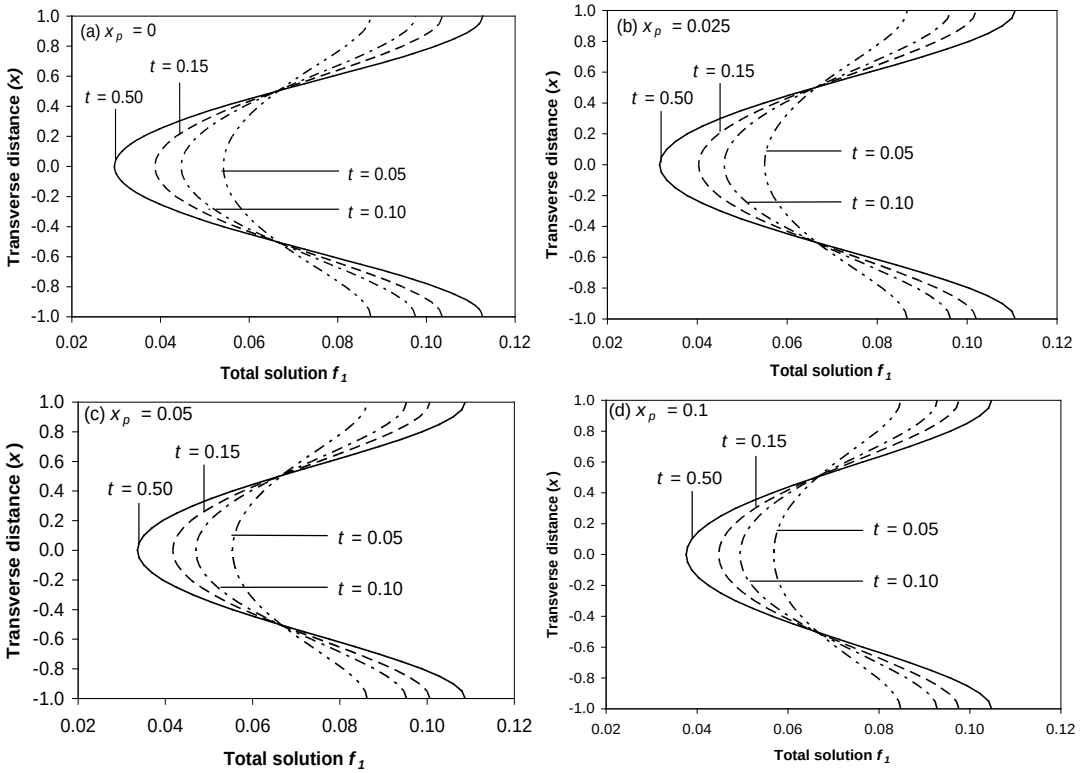

Figure 7: Distribution of total solution f_1 at different instants of time t for dispersion in a channel with (a) $x_p = 0.0$, (b) $x_p = 0.025$, (c) $x_p = 0.05$ and (d) $x_p = 0.1$.

The evolution of the dispersion function with time for solutes dispersion in flow through pipe and channel, for different fluid models is depicted in Figs. 8(a) and 8(b) respectively. It is clear that the magnitude of the dispersion function f_1 is considerably higher when the solute disperses in H-B fluid flow than it disperses in Casson fluid flow. It is also clear that the magnitude of dispersion is higher when the solute disperses in pipe than when it disperses in channel. Figs. 6-8 bring out the evolution of the total solution of dispersion function f_1 over time and the non-Newtonian effects of the solvent fluid through which the solute disperses.

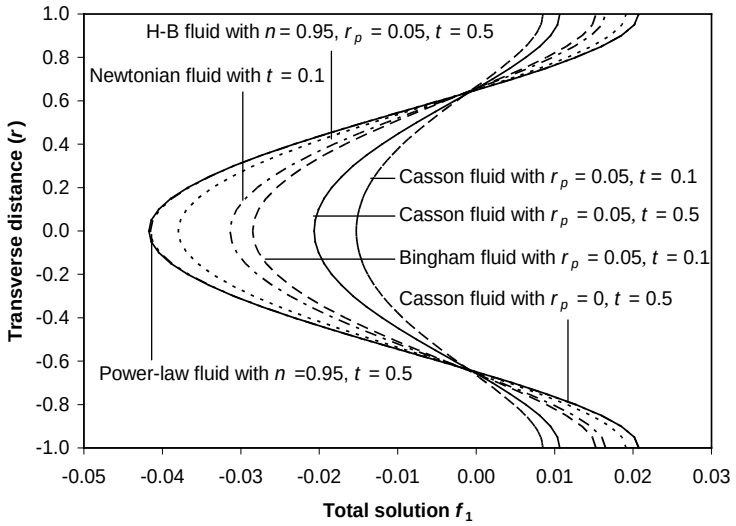

(a) Flow in a pipe.

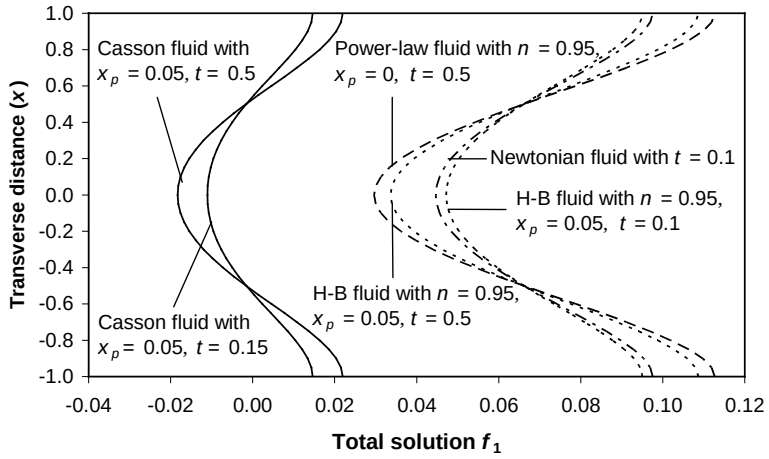

(b) Flow in a channel.

Figure 8: Distribution of total solution f_1 for different fluid models in (a) pipe and (b) channel.

3.4 Mean concentration

Mean concentration C_m of the solute is a physiologically important flow measurement which is useful to find the concentration of the fluid C ultimately. Variation of the mean concentration C_m of the solute with time t for different values of the solute length parameter z_s with $z = 0.5$, $n = 0.95$, $r_p = x_p = 0.1$ and $Pe = \sqrt{48}$ when the solute disperses in pipe and channel is depicted in Figs. 9(a) and 9(b), respectively. It is observed that in both the cases of solutes dispersion in pipe and channel, the mean concentration of the solute increases rapidly when time t increases

from 0 to 1 and then it decreases rapidly when time t increases from 1 to 2. The mean concentration decreases slowly when time t increases further from 2 to 5 for the flow in pipe, and it decreases slowly when time t increases further from 2 to 3 for the flow in channel. It is also noted that the mean concentration of solute increases considerably with the increase of length of the solute when the solute disperses through either pipe or channel. It is found that at any instant of time, the mean concentration of the solute is marginally higher when it disperses in pipe than when it disperses in channel.

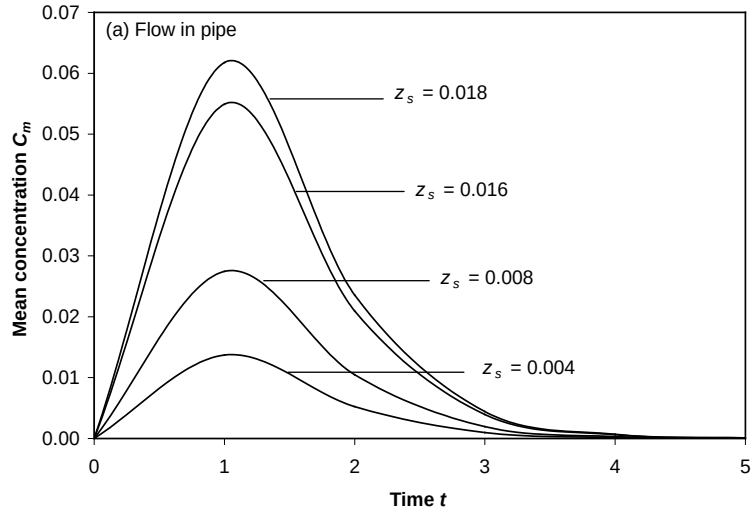

(a) Flow in pipe

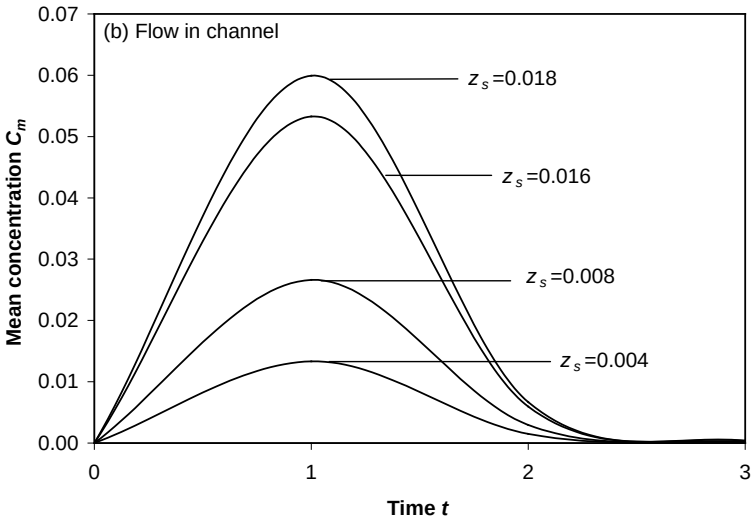

(b) Flow in channel

Figure 9: Variation of the mean concentration of the solute with time t for different values of z_s with $z = 0.5$, $n = 0.95$, $r_p = x_p = 0.1$ and $Pe = \sqrt{48}$ when the solute disperses in (a) pipe and (b) channel.

Fig. 10 illustrates the variation of mean concentration of the solute with time when it disperses through different fluids in pipe and channel with $z = 0.5$, $n = 0.95$, $r_p = x_p = 0.1$, $Pe = \sqrt{48}$ and $z_s = 0.004$. It is found that at any instant of time, the mean concentration of the solute is marginally higher when it disperses in the flow through pipe than when it disperses in the flow through channel. One can also observe that at any instant of time, the mean concentration of the solutes is considerably higher when it disperses in H-B fluid than when it disperses in Casson fluid.

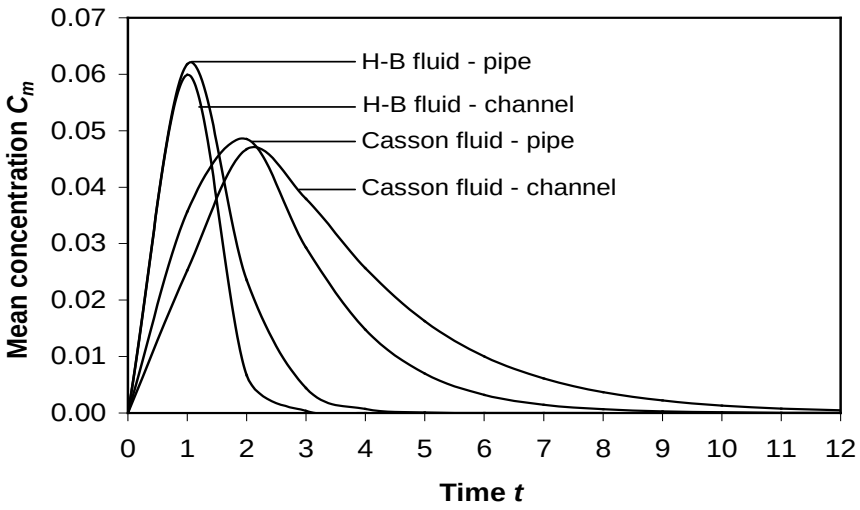

Figure 10: Variation of mean concentration of the solute with time when it disperses through different fluids in pipe and channel with $z = 0.5$, $n = 0.95$, $r_p = x_p = 0.1$, $Pe = \sqrt{48}$ and $z_s = 0.004$.

3.5 Quantification of flow measurements

From Figs. 2 and 3, it is clear that both in the cases of flow through pipe and channel, the dispersion of the solute and mean velocity of the solvent (H-B) fluid decrease considerably with the increase of the yield stress of H-B fluid at a constant pressure gradient. The estimates of the percentage of decrease in the dispersion coefficient, mean velocity and relative axial diffusivity for H-B and Casson fluid models for different values of radius$\left(r_p\right)$/semi width$\left(x_p\right)$ of the plug core region and power-law index n in the steady dispersion of solutes in flow through pipe and channel are computed in Table 1 and Table 2, respectively. It is recorded that the estimates of the percentage of decrease in each of the aforesaid estimates increases marginally with the increase of the power-law index n and increases significantly (nonlinearly) with the increase of the radius/semi width of the plug flow region. Since the radius/semi width of the plug core region entirely depends on the yield stress of the flowing fluid, the increase in the yield stress value of the H-B/Casson fluids increases significantly in each of the aforesaid estimates in the dispersion of solute in flow through either

pipe or channel. It is also found that the estimates of the percentage of decrease in dispersion of solutes, mean velocity and relative axial diffusivity are considerably lower in flow through pipe than the corresponding estimates obtained for the dispersion of solutes in flow through channel.

Table 1: Estimates of the percentage of decrease in the dispersion coefficient, mean velocity and relative effective diffusivity in the steady dispersion of solutes in H-B and Casson fluids flow through pipe for different values of radius of the plug core region and power-law index *n*.

r_p	Dispersion coefficient				Mean velocity				Effective axial diffusivity			
	H-B fluid			Casson fluid	H-B fluid			Casson fluid	H-B fluid			Casson fluid
	n = 0.95	n = 1	n = 1.05		n = 0.95	n = 1	n = 1.05		n = 0.95	n = 1	n = 1.05	
0.02	6.32	6.59	6.86	54.45	2.55	2.67	2.79	29.50	1.36	1.40	1.45	8.35
0.04	12.44	12.95	13.46	68.75	5.10	5.33	5.57	40.24	2.78	2.87	2.96	12.50
0.06	18.35	19.09	19.80	77.16	7.65	8.00	8.35	47.87	4.27	4.40	4.53	15.97
0.08	24.07	24.99	25.88	82.79	10.21	10.67	11.12	53.87	5.83	6.01	6.19	19.13
0.10	29.58	30.66	31.71	86.81	12.76	13.33	13.89	58.86	7.46	7.69	7.90	22.10
0.12	34.88	36.09	37.27	89.78	15.33	15.99	16.65	63.10	9.17	9.44	9.70	24.93
0.14	39.96	41.28	42.56	92.02	17.89	18.65	19.41	66.78	10.95	11.27	11.58	27.68
0.16	44.82	46.24	47.60	93.75	20.45	21.31	22.15	70.03	12.80	13.17	13.53	30.36
0.18	49.46	50.94	52.36	95.08	23.02	23.96	24.90	72.92	14.73	15.15	15.55	32.98
0.20	53.87	55.41	56.86	96.13	25.58	26.61	27.63	75.50	16.73	17.20	17.65	35.55

Table 2: Estimates of the percentage of decrease in the dispersion coefficient, mean velocity and relative effective diffusivity in the steady dispersion of solutes in H-B and Casson fluids flow through channel for different values of semi-width of the plug core region and power-law index *n*.

x_p	Dispersion coefficient				Mean velocity				Effective axial diffusivity			
	H-B fluid			Casson fluid	H-B fluid			Casson fluid	H-B fluid			Casson fluid
	n = 0.95	n = 1	n = 1.05		n = 0.95	n = 1	n = 1.05		n = 0.95	n = 1	n = 1.05	
0.02	7.44	7.72	7.98	57.24	2.88	3.00	3.12	30.93	1.86	1.92	1.97	10.37
0.04	14.59	15.10	15.60	71.53	5.76	6.00	6.23	41.99	3.83	3.92	4.02	15.38
0.06	21.44	22.15	22.85	79.71	8.64	8.99	9.34	49.78	5.87	6.01	6.15	19.53
0.08	27.97	28.85	29.71	85.06	11.51	11.97	12.43	55.88	7.99	8.18	8.35	23.25
0.10	34.17	35.20	36.18	88.79	14.39	14.95	15.50	60.89	10.19	10.41	10.63	26.70
0.12	40.06	41.19	42.28	91.50	17.25	17.91	18.56	65.15	12.44	12.72	12.98	29.94
0.14	45.61	46.82	47.98	93.49	20.11	20.86	21.60	68.82	14.77	15.09	15.39	33.03
0.16	50.82	52.10	53.32	95.00	22.95	23.80	24.62	72.03	17.15	17.51	17.85	36.01
0.18	55.71	57.02	58.27	96.14	25.78	26.71	27.61	74.87	19.58	19.99	20.37	38.88
0.20	60.27	61.60	62.86	97.02	28.60	29.60	30.58	77.41	22.06	22.51	22.95	41.66

3.6 Some possible clinical applications

The estimates of the dispersion coefficient, mean velocity and relative axial dispersion obtained in Table 1 are physiologically important flow quantities [26]. For the physiological data of the canine vascular system [14, 17], the estimates of the aforesaid flow measurements in the dispersion of solutes in H-B and Casson fluids flow through pipe and channel are computed in Table 3 and Table 4, respectively. It is observed that in the dispersion of solutes in flow through circular pipe, the estimates of the dispersion coefficient, mean velocity relative axial diffusivity decrease considerably with the increase of the plug core radius r_p. One can noticed that the dispersion coefficient and the mean velocity decrease marginally with the increase of the power-law index n except for dispersion coefficient in venules and arterioles which is increases marginally with the increase of power-law index *n*. It is also clear that the relative effective axial diffusivity increases marginally with the increase of the power-law index *n.* In the case of dispersion of solutes in the flow through channel, the estimates of the aforesaid flow measurements decrease with the increase of the power-law index. It is also noticed that the estimates of these flow measurements are considerably higher in the dispersion of solutes in H-B fluid flow than those in the dispersion of solutes in Casson fluid flow. It is recorded that the estimates of these flow measurements are considerably higher in the dispersion of solutes in flow through circular pipe than the corresponding estimates obtained from the dispersion of solutes in the flow through channel for the inferior vena cava, venules and arterioles but considerably lower in the ascending aorta.

Table 3: Estimates of dispersion coefficient, mean velocity and relative axial diffusivity in the dispersion of solutes in pipe flow at $t = 0.1$ for the canine vascular systems.

Artery type	Velocity (cm/s)	Diameter (cm)	r_p	Dispersion coefficient				Mean velocity				Relative axial diffusivity			
				n = 0.95	n = 1	n = 1.05	Casson fluid	n = 0.95	n = 1	n = 1.05	Casson fluid	n = 0.95	n = 1	n = 1.05	Casson fluid
Ascending aorta	20.00	1.500	0.0737	0.62	0.61	0.61	0.15	0.91	0.90	0.89	0.48	0.75	0.75	0.76	0.64
Inferior vena cava	25.00	1.000	0.0392	0.69	0.69	0.69	0.25	0.95	0.95	0.95	0.59	0.77	0.77	0.77	0.68
Venules	0.35	0.004	0.0112	0.76	0.77	0.77	0.44	0.99	0.98	0.98	0.77	0.78	0.79	0.79	0.73
Arterioles	0.75	0.005	0.0065	0.77	0.78	0.78	0.51	0.99	0.99	0.99	0.82	0.79	0.79	0.79	0.74

Table 4: Estimates of dispersion coefficient, mean velocity and relative axial diffusivity in the dispersion of solutes in channel flow at $t = 0.1$ for the canine vascular systems.

Artery type	Velocity (cm/s)	Diameter (cm)	x_p	Dispersion coefficient				Mean velocity				Relative axial diffusivity			
				$n = 0.95$	$n = 1$	$n = 1.05$	Casson fluid	$n = 0.95$	$n = 1$	$n = 1.05$	Casson fluid	$n = 0.95$	$n = 1$	$n = 1.05$	Casson fluid
Ascending aorta	20.0	1.500	0.0737	0.62	0.62	0.610	0.11	0.99	0.99	0.99	0.46	0.63	0.63	0.63	0.49
Inferior vena cava	25.0	1.000	0.0390	0.55	0.54	0.533	0.11	0.94	0.94	0.94	0.58	0.62	0.61	0.61	0.31
Venules	0.35	0.004	0.0112	0.61	0.62	0.601	0.34	0.98	0.98	0.98	0.76	0.63	0.63	0.62	0.59
Arterioles	0.75	0.005	0.0065	0.62	0.62	0.612	0.39	0.99	0.99	0.99	0.82	0.63	0.63	0.63	0.59

4. Conclusion

This mathematical analysis brings out many interesting and useful results on the unsteady dispersion of solutes in blood flow through (i) pipe and (ii) channel, modeling blood as H-B fluid model and the results of this study are compared with the results of Dash et al. [26]. The major findings of this mathematical model are summarized below.

(i) For flow in pipe/channel, the dispersion coefficient, relative effective diffusivity and magnitude of the dispersion function decrease considerably with the increase of the yield stress of H-B/Casson fluid and power-law index of H-B fluid.

(ii) The dispersion coefficient, relative effective diffusivity and magnitude of the dispersion function are considerably higher when the solute disperses in pipe than when it disperses in channel.

(iii) For the solutes dispersion in the flow through pipe/channel, the dispersion coefficient, relative effective diffusivity and magnitude of the dispersion function are considerably higher when the solute disperses in H-B fluid than when it disperses in Casson fluid.

(iv) The estimates of the percentage of decrease in the dispersion coefficient and effective axial diffusivity increase significantly with the increase of yield stress of the H-B/Casson fluid, and are significantly lower when the solute disperses in H-B fluid than when it disperses in Casson fluid. These estimates are lower when the solute disperses in the flow through pipe than when it disperses in the flow through channel.

From the results obtained in this study, we observe that there is a substantial difference between the flow quantities of H-B fluid model (present results) and Casson fluid model [26] and thus, one can expect that the present H-B fluid model may be useful in predicting the physiologically important flow quantities with better accuracy. Hence, it is conclude that the present mathematical analysis may be considered as an improvement in the mathematical modeling of unsteady dispersion of solutes in blood flow through narrow arteries. Since blood flow in narrow arteries is highly pulsatile in nature, the study on the unsteady dispersion of solutes in pulsatile flow of blood would be more realistic and this will be taken up in the near future.

Acknowledgment

The authors thank GSR, UTB for supporting this research work through a internal research grant Ref. No.: UTB/GSR/1/2015 (5). The authors also thank Universiti Sains Malaysia, Malaysia for supporting this research work through Research University grant (RU Grant ref. no: 1001/PMATHS/811177).

References

[1] Kuehn, T. H., and Goldstein, R. J., 1976, "An experimental and theoretical study of natural convection in the annulus between horizontal concentric cylinders," J. Fluid Mech. 4, pp. 695-719.

[2] Mercer, G. N., and Roberts, A. J., 1990, "A centre manifold description of contaminant dispersion in channels with varying properties," SIAM J. Appl. Math., 50, pp. 1547-1565.

[3] DeCarli, J. P., 1990, "Displacement separations by continuous annular chromatography," AIChE J., 36, pp. 1220-1228.

[4] Tsui, Y. T., and Tremblay, 1984**,** "On transient natural convection heat transfer in the annulus between concentric, horizontal cylinders with isothermal surfaces," Int. J. Heat and Mass Trans., 27, pp. 103-111.

[5] Jiang, Y., and Grotberg, J. B., 1993, "Bolus contaminant dispersion in oscillatory tube flow with conductive walls," ASME Trans. J. Biomech. Engng., 115, pp. 424-431.

[6] Carta, G., DeCarli, J. P., Byers, C. H., and Sisson, W. G., 1989, "Separation of metals by continuous annular chromatography with step elution," Chem. Eng. Commun., 79, pp. 207-227.

[7] Bloomingburg, G. F., and Carta, G., 1994, "Separation of protein mixtures by annular chromatography with step elution," Chem. Eng. J., 55, pp. B19-B27.

[8] Taylor, G. I., 1953, "Dispersion of soluble matter in solvent flowing slowly through a tube," Proc. R. Soc. London, Series A., 219, pp. 186-203.

[9] Aris, R., 1956, "On the dispersion of a solute in a fluid flowing through a tube," Proceedings of the Royal Society London. Series A, 235, pp. 66-77.

[10] Ananthakrishnan, V., Gill, W. N., Barduhn, A. J., 1965, "Laminar dispersion in capillaries: Part I. Mathematical Analysis," AIChE J., 11, pp. 1063-1072.

[11] Gill, W. N., 1967, "A note on the solution of transient dispersion problems," Proceedings of the Royal Society A: Mathematical, Physical and Engineering Sciences, 298, pp. 335-339.

[12] Gill, W. N., and Sankarasubramanian, R., 1970, "Exact analysis of unsteady convective diffusion", Proceedings of the Royal Society A: Mathematical, Physical and Engineering Sciences, 316, pp. 341-350.

[13] Sankarasubramanian, R., and Gill, W. N., 1973, "Unsteady convective diffusion with interphase mass transfer," Proceedings of the Royal Society A: Mathematical, Physical and Engineering Science, 333, pp. 115-132.

[14] Sharp, M. K., 1993, "Shear-augmented dispersion in non-Newtonian fluids," Ann. Biomed. Eng., 21, pp. 407-415.

[15] Philips, C. G., Kaye, S. R., and Robinson, C. D., 1995, "Time dependent transport by convection and diffusion with exchange between two phases," J. Fluid Mech., 297, pp. 373-401.

[16] Ramana1, B., Sarojamma, G., Vishali, B., and Nagarani, P., 2012, "Dispersion of a solute in a Herschel-Bulkley fluid flowing in a conduit," J. Experimental Sci., 3, pp. 14-23.

[17] Sankar, D. S., Jaafar, N. A., Yazariah Y., 2012, "Nonlinear analysis for shear augmented dispersion of solutes in blood through narrow arteries," J. Appl. Math. Vol. 2012, Article ID 812535, DOI:10.1155/2012/812535.

[18] Tu, C., and Deville, M., 1996, "Pulsatile flow of non-Newtonian fluids through arterial stenoses," J. Biomech., 29, pp. 899-908.

[19] Sankar, D. S., Yazariah, Y. 2012, "Comparative analysis of mathematical models for blood flow in tapered constricted arteries," Abstracts and Applied Analysis Vol. 2012, Article ID: 235960, DOI: 10.1155/2012/235960.

[20] Dash, R. K., Jayaraman, G., and Metha, K. N., 1996, "Estimation of increased flow resistance in a narrow catheterized artery-A theoretical model," J. Biomech., 29, pp. 917-930.

[21] Sankar, D. S., and Karim, M. F., "Influence ofbodyacceleration in blood flow through narrow arteries with multiple constrictions," IET Digital Library, Proc. of 5th Brunei International Conference on Engineering and Technology, Nov. 1-3, 2014, pp. 1-14. (ISBN: 978-84929-991-9; Conf. No.: CP469).

[22] Scott Blair, G. W., 1966, "The success of Casson's equatio," Rheologica Acta, 5, pp. 184-187.

[23] Scott Blair, G. W., and Spanner, D. C., An Introduction to Biorheology, Elsevier Scientific Publishing Co., Amsterdam (1974).

[24] Chaturani, P., and Ponnalagar Samy, R., 1985, "A study of non-Newtonian aspects of blood flow through stenosed arteries and its applications in arterial diseases," Biorheology, 22, pp. 521-531.

[25] Iida, N., 1978, "Influence of plasma layer on steady blood flow in microvessels," Jap. J. Appl. Phys., 17, pp. 203-214.

[26] Dash, R. K., Jayaraman, G., and Metha, K. N., 2000, "Shear augmented dispersion of a solute in a Casson fluid flowing in a conduit," Annals of Biomedical Engg., 28, pp. 373-380.

[27] Sharp, M. K., Kamm, R. D., Shapiro, A. H., Karniadakis, G., and Kimmel, E., 1991, "Dispersion in a curved tube during oscillatory flow," J. Fluid Mech. 223, pp. 537-563.

Appendix A

The expression obtained after evaluating the integrals I_1 and I_2 appearing in the expression of f_{1t} (for flow in pipe) are given below.

$$I_1=\frac{1}{1238630400}\left[\frac{1}{2(n+3)}-\frac{(n+1)r_p}{2(n+2)}+\frac{nr_p^2}{4}-\frac{(n-1)n\,r_p^{n+1}}{8}-\frac{\left(n^4+2n^3-5n^2-6n+4\right)r_p^{n+3}}{8(n+2)(n+3)}\right]$$

$$\times\left[-6r_p^{12}\lambda_m^{10}+700r_p^{10}\lambda_m^8-53760r_p^8\lambda_m^6+2419200r_p^6\lambda_m^4-51609600r_p^4\lambda_m^2+309657600r_p^2\right]r_p^2\;r^2$$

$$+\left(-\frac{r_p^{12}\lambda_m^{10}}{176947200}+\frac{r_p^{10}\lambda_m^8}{1474560}-\frac{r_p^8\lambda_m^6}{18432}+\frac{r_p^6\lambda_m^4}{384}-\frac{r_p^4\lambda_m^2}{16}+\frac{r_p^2}{2}\right)CI \qquad \text{(A1)}$$

$$I_2=\left[-\frac{\left(n^4+2n^3-5n^2-6n+4\right)\lambda_m^1}{8493465600\left(n^2+5n+6\right)}+\frac{\left(n^4+2n^3-5n^2-6n+4\right)\lambda_m^8}{58982400\left(n^2+5n+6\right)}-\frac{\left(n^4+2n^3-5n^2-6n+4\right)\lambda_m^6}{589824\left(n^2+5n+6\right)}\right.$$

$$\left.+\frac{\left(n^4+2n^3-5n^2-6n+4\right)\lambda_m^4}{9216\left(n^2+5n+6\right)}-\frac{\left(n^4+2n^3-5n^2-6n+4\right)\lambda_m^2}{256\left(n^2+5n+6\right)}+\frac{\left(n^4+2n^3-5n^2-6n+4\right)}{16\left(n^2+5n+6\right)}\right]r_p^{n+3}$$

$$-\frac{\left(n^4+2n^3-5n^2-6n+4\right)r_p^{n+5}}{16\left(n^2+5n+6\right)}$$

$$-\frac{\left(\begin{array}{l}\left(n^4+2n^3-5n^2-6n+4\right)\log(r_p)(r_p^{10}\lambda_m^{10}-120r_p^8\lambda_m^8+9600r_p^6\lambda_m^6\\-460800r_p^4\lambda_m^4+11059200r_p^2\lambda_m^2-88473600\end{array}\right)r_p^{n+5}}{707788800\left(n^2+5n+6\right)}$$

$$+\frac{\left(n^4+2n^3-5n^2-6n+4\right)\lambda_m^2\;r_p^{n+7}}{256\left(n^2+5n+6\right)}-\frac{\left(n^4+2n^3-5n^2-6n+4\right)\lambda_m^4\;r_p^{n+9}}{9216\left(n^2+5n+6\right)}+\frac{\left(n^4+2n^3-5n^2-6n+4\right)\lambda_m^6\;r_p^{n+1}}{589824\left(n^2+5n+6\right)}$$

$$-\frac{\left(n^4+2n^3-5n^2-6n+4\right)\lambda_m^8\;r_p^{n+13}}{58982400\left(n^2+5n+6\right)}+\frac{\left(n^4+2n^3-5n^2-6n+4\right)\lambda_m^{10}r_p^{n+15}}{8493465600\left(n^2+5n+6\right)}$$

$$+\frac{1}{29491200(n+1)}\left[n\left(\frac{\lambda_m^{10}}{(n+13)}-\frac{100\lambda_m^8}{(n+11)}+\frac{6400\lambda_m^6}{(n+9)}-\frac{230400\lambda_m^4}{(n+7)}+\frac{3686400\lambda_m^2}{(n+5)}-\frac{14745600}{(n+3)}\right)r_p^2\right]$$

$$+\frac{1}{14745600(n+2)^2}\left[(n+1)\left(-\frac{\lambda_m^{10}}{(n+14)}+\frac{100\lambda_m^8}{(n+15)}-\frac{6400\lambda_m^6}{(n+10)}+\frac{230400\lambda_m^4}{(n+8)}-\frac{3686400\lambda_m^2}{(n+6)}+\frac{14745600}{(n+4)}\right)r_p\right]$$

$$+\left(\frac{\left(n^4+2n^3-5n^2-6n+4\right)r_p^{n+3}}{8(n+2)(n+3)}+\frac{n\,r_p^2}{4}-\frac{(n+1)r_p}{2(n+2)}+\frac{1}{2(n+3)}\right)\left(-\frac{\lambda_m^{10}}{206438400}+\frac{\lambda_m^8}{1769472}\right.$$

$$\left.-\frac{\lambda_m^6}{23040}+\frac{\lambda_m^4}{512}-\frac{\lambda_m^2}{24}+\frac{1}{4}\right)+\frac{1}{14745600(n+3)^2}\left[\left(\frac{\lambda_m^{10}}{(n+14)}-\frac{100\lambda_m^8}{(n+15)}+\frac{6400\lambda_m^6}{(n+10)}-\frac{230400\lambda_m^4}{(n+8)}\right.\right.$$

$$\left.\left.+\frac{3686400\,\lambda_m^2}{(n+6)}-\frac{14745600}{(n+4)}\right)\right]+\left(\frac{\left(n^4+2n^3-5n^2-6n+4\right)}{4(n+2)(n+3)}r_p^{n+3}log\left(r_p\right)\right)\left(\frac{\lambda_m^{10}\,r_p^{12}}{176947200}-\frac{\lambda_m^8\;r_p^{10}}{1474560}\right.$$

$$+\frac{\lambda_m^6 r_p^8}{18432}-\frac{\lambda_m^4 r_p^6}{384}+\frac{\lambda_m^2 r_p^4}{16}-\frac{r_p^2}{2}-\frac{\lambda_m^{10}}{176947200}+\frac{\lambda_m^8}{1474560}-\frac{\lambda_m^6}{18432}+\frac{\lambda_m^4}{384}-\frac{\lambda_m^2}{16}+\frac{1}{2}\Bigg)$$

$$+\left(\frac{(n^7+10n^6+32n^5+18n^4-93n^3-164n^2-52n+40)r_p^{n+3}}{8(n+1)(n+2)^2(n+3)^2}\right)\left(\frac{\lambda_m^{10} r_p^{12}}{176947200}-\frac{\lambda_m^8 r_p^{10}}{1474560}+\frac{\lambda_m^6 r_p^8}{18432}\right.$$

$$\left.-\frac{\lambda_m^4 r_p^6}{384}+\frac{\lambda_m^2 r_p^4}{16}-\frac{r_p^2}{2}-\frac{\lambda_m^{10}}{176947200}+\frac{\lambda_m^8}{1474560}-\frac{\lambda_m^6}{18432}+\frac{\lambda_m^4}{384}-\frac{\lambda_m^2}{16}+\frac{1}{2}\right)$$

$$+CI\left(\frac{\lambda_m^{10} r_p^{12}}{176947200}-\frac{\lambda_m^8 r_p^{10}}{1474560}+\frac{\lambda_m^6 r_p^8}{18432}-\frac{\lambda_m^4 r_p^6}{384}+\frac{\lambda_m^2 r_p^4}{16}-\frac{r_p^2}{2}-\frac{\lambda_m^{10}}{176947200}+\frac{\lambda_m^8}{1474560}\right.$$

$$\left.-\frac{\lambda_m^6}{18432}+\frac{\lambda_m^4}{384}-\frac{\lambda_m^2}{16}+\frac{1}{2}\right)-\left(\frac{1}{2(n+3)}-\frac{(n+1)r_p}{2(n+2)}+\frac{n r_p^2}{4}+\frac{(n^4+2n^3-5n^2-6n+4)r_p^{n+3}}{8(n+2)(n+3)}\right)$$

$$\times\left(-\frac{\lambda_m^{10} r_p^{14}}{206438400}+\frac{\lambda_m^8 r_p^{12}}{1769472}-\frac{\lambda_m^6 r_p^{10}}{23040}+\frac{\lambda_m^4 r_p^8}{512}-\frac{\lambda_m^2 r_p^6}{24}+\frac{r_p^4}{4}\right)$$

$$-\frac{1}{14745600(n+3)^2}\left(-\frac{14745600 r_p^{n+4}}{(n+4)}+\frac{3686400\lambda_m^2 r_p^{n+6}}{(n+6)}-\frac{230400\lambda_m^4 r_p^{n+8}}{(n+8)}+\frac{6400\lambda_m^6 r_p^{n+10}}{(n+10)}+\frac{\lambda_m^{10} r_p^{n+14}}{(n+14)}\right.$$

$$\left.-\frac{100\lambda_m^8 r_p^{n+15}}{(n+15)}\right)-\frac{1}{29491200(n+1)}\left[n\left(-\frac{14745600 r_p^{n+5}}{(n+3)}+\frac{3686400\lambda_m^2 r_p^{n+7}}{(n+5)}-\frac{230400\lambda_m^4 r_p^{n+9}}{n+7}\right.\right.$$

$$\left.\left.+\frac{6400\lambda_m^6 r_p^{n+11}}{(n+9)}-\frac{100\lambda_m^8 r_p^{n+13}}{(n+11)}+\frac{\lambda_m^{10} r_p^{n+15}}{(n+13)}\right)\right]-\frac{1}{14745600(n+2)^2}\left[(n+1)\left(\frac{14745600 r_p^{n+5}}{(n+4)}\right.\right.$$

$$\left.\left.-\frac{3686400\lambda_m^2 r_p^{n+7}}{(n+6)}+\frac{230400\lambda_m^4 r_p^{n+9}}{(n+8)}-\frac{6400\lambda_m^6 r_p^{n+11}}{(n+10)}-\frac{\lambda_m^{10} r_p^{n+15}}{(n+14)}+\frac{100\lambda_m^8 r_p^{n+16}}{(n+15)}\right)\right] \quad \text{(A2)}$$

Appendix B

The expression for $K_2(t)$ in the case of flow in pipe is given below.

$$K_2(t)=\frac{1}{Pe^2}+(1/192)\left[\frac{96(n+1)^2}{(n+3)^3(n+5)}-\frac{192n(n+1)^2(2n+9)r_p}{(n+2)(n+3)(n+4)(n+5)(2n+5)}\right.$$

$$+\frac{96n(n+1)\left(2n^5+23n^4+90n^3+128n^2+13n-64\right)r_p^2}{(n+2)^3(n+3)^2(n+4)(n+5)}-\frac{96(n-1)n^2(n+1)(2n+7)r_p^3}{(n+2)(n+3)(n+4)(2n+3)}$$

$$+\frac{24(n-1)^2n^2r_p^4}{(n+1)(n+3)}-\frac{48(n+1)(n+7)\left(n^4+2n^3-5n^2-6n+4\right)r_p^{n+3}}{(n+2)(n+3)^3(n+5)}$$

$$+\frac{48n(n+1)(n+6)\left(n^4+2n^3-5n^2-6n+4\right)r_p^{n+4}}{(n+2)^3(n+3)(n+4)}$$

$$-\frac{24}{(n+1)(n+2)(n+3)^2(n+4)(n+5)}\begin{pmatrix}n^9+15n^8+70n^7+46n^6-411n^5-597n^4\\+740n^3+920n^2-496n-96\end{pmatrix}r_p^{n+5}$$

$$-\frac{48(n+1)^2\left(n^4+6n^3-3n^2-36n+24\right)r_p^{n+6}}{(n+2)(n+3)(n+4)(n+5)}+\frac{24n(n+1)\left(n^4+6n^3-3n^2-36n+24\right)r_p^{n+7}}{(n+3)(n+4)(n+5)}$$

$$-\frac{12\begin{pmatrix}4n^{13}+48n^{12}+195n^{11}+160n^{10}-913n^9-1878n^8+1865n^7+6772n^6-2535n^5\\-18918n^4-12512n^3+5656n^2+4872n-1152\end{pmatrix}r_p^{2n+6}}{(n+1)(n+2)^3(n+3)^3(2n+3)(2n+5)}$$

$$\left.+\frac{12(n+1)\left(n^4+2n^3-5n^2-6n+4\right)\left(n^4+6n^3-3n^2-36n+24\right)r_p^{2n+8}}{(n+2)(n+3)^2(n+4)(n+5)}-\frac{24\left(n^4+2n^3-5n^2-6n+4\right)^2r_p^{2n+6}lo\ \left(r_p\right)}{(n+2)^2(n+3)^2}\right]$$

$$-2\left\{A_m\left(\frac{\left(n^4+2n^3-5n^2-6n+4\right)rp^{n+3}}{2(n+2)(n+3)}-\frac{(n-1)nrp^{n+1}}{2}+nrp^2-\frac{2(n+1)rp}{(n+2)}+\frac{2}{(n+3)}\right)\right.$$

$$\times e^{-\lambda_m^2t}\left(-\frac{rp^{16}\lambda_n^{14}}{6658877030400}+\frac{rp^{14}\lambda_m^{12}}{29727129600}-\frac{rp^{12}\lambda_m^{10}}{176947200}+\frac{rp^{10}\lambda_m^8}{1474560}-\frac{rp^8\lambda_m^6}{18432}+\frac{rp^6\lambda_m^4}{384}-\frac{rp^4\lambda_m^2}{16}+\frac{rp^2}{2}\right)$$

$$+\frac{1}{294912}A_me^{-\lambda_m^2t}\left[2\left(\frac{\lambda_m^8r_p^{11}}{(n+11)}-\frac{64\lambda_m^6r_p^9}{(n+9)}+\frac{2304\lambda_m^4r_p^7}{(n+7)}-\frac{36864\lambda_m^2r_p^5}{(n+5)}+\frac{147456r_p^3}{(n+3)}\right)r_p^n\right.$$

$$-2(n+1)\left(\frac{\lambda_m^8r_p^{10}}{(n+10)}-\frac{64\lambda_m^6r_p^8}{(n+8)}+\frac{2304\lambda_m^4r_p^6}{(n+6)}-\frac{36864\lambda_m^2r_p^4}{(n+4)}+\frac{147456r_p^2}{(n+2)}\right)r_p^{n+1}$$

$$\left.+\frac{\left(n^4+2n^3-5n^2-6n+4\right)}{(n+2)(n+3)}\left(\frac{\lambda_m^8}{10}-8\lambda_m^6+384\lambda_m^4-9216\lambda_m^2+73728\right)r_p^{n+3}\right.$$

$$
-\frac{\left(n^4+2n^3-5n^2-6n+4\right)\left(r_p^8\lambda_m^8-80r_p^6\lambda_m^6+3840r_p^4\lambda_m^4-92160r_p^2\lambda_m^2+737280\right)r_p^{n+5}}{10\left(n+2\right)\left(n+3\right)}
$$

$$
+\frac{2\left(n+1\right)\left(r_p^8\lambda_m^8-80r_p^6\lambda_m^6+3840r_p^4\lambda_m^4-92160r_p^2\lambda_m^2+737280\right)r_p^3}{5\left(n+2\right)}
$$

$$
-\frac{4}{5}\left(n-1\right)n\lambda_m^2\left(\frac{\lambda_m^6}{\left(n+9\right)}-\frac{60\lambda_m^4}{\left(n+7\right)}+\frac{1920\lambda_m^2}{\left(n+5\right)}-\frac{23040}{\left(n+3\right)}\right)r_p^2
$$

$$
+n\left[\left(\frac{\left(n+1\right)\lambda_m^8r_p^9}{\left(n+9\right)}-\frac{64\left(n+1\right)\lambda_m^6r_p^7}{\left(n+7\right)}+\frac{2304\left(n+1\right)\lambda_m^4r_p^5}{\left(n+5\right)}-\frac{36864\left(n+1\right)\lambda_m^2r_p^3}{\left(n+3\right)}+147456r_p\right)r_p^n\right.
$$

$$
\left.-\frac{1}{5}\lambda_m^8r_p^{10}+16\lambda_m^6r_p^8-768\lambda_m^4r_p^6+18432\lambda_m^2r_p^4-147456r_p^2\right]r_p^2
$$

$$
-\frac{4\left(n+1\right)}{\left(n+2\right)}\left(\frac{\lambda_m^8}{10}-8\lambda_m^6+384\lambda_m^4-9216\lambda_m^2+73728\right)r_p
$$

$$
+2\left(n+1\right)\left(\frac{\lambda_m^8}{\left(n+10\right)}-\frac{64\lambda_m^6}{\left(n+8\right)}+\frac{2304\lambda_m^4}{\left(n+6\right)}-\frac{36864\lambda_m^2}{\left(n+4\right)}+\frac{147456}{\left(n+2\right)}\right)r_p
$$

$$
-\frac{2\lambda_m^8}{\left(n+11\right)}+\frac{128\lambda_m^6}{\left(n+9\right)}-\frac{4608\lambda_m^4}{\left(n+7\right)}+\frac{73728\lambda_m^2}{\left(n+5\right)}+\frac{4}{\left(n+3\right)}\left(\frac{\lambda_m^8}{10}-8\lambda_m^6+384\lambda_m^4-9216\lambda_m^2+73728\right)
$$

$$
\left.-\frac{4}{\left(n+3\right)}\left(\frac{1}{10}\lambda_m^8r_p^{10}-8\lambda_m^6r_p^8+384\lambda_m^4r_p^6-9216\lambda_m^2r_p^4+73728r_p^2\right)-\frac{294912}{\left(n+3\right)}\right]\Bigg\} \quad \text{(B1)}
$$

Appendix C

The expression for $K_2(t)$ in the case of flow in channel is given below.

$$K_2(t)=\frac{1}{Pe^2}+\frac{8}{945}\left(\frac{315(n+1)^2}{4(n+2)^2(n+4)(2n+5)}-\frac{315n(n+1)(2n+7)x_p}{8(n+2)^2(n+3)(n+4)}+\frac{315\left(n^4+6n^3+8n^2-3n-3\right)x_p^2}{4(n+2)^2(n+3)(n+4)}\right.$$
$$-\frac{315(n-1)n(2n+5)x_p^3}{16(n+2)(n+3)}+\frac{315(n-1)^2(n+1)^2x_p^4}{16(n+2)(2n+1)}-\frac{315n(n+1)(n+6)\left(n^2-3\right)x_p^{n+2}}{16(n+2)^2(n+3)(n+4)}$$
$$+\frac{315n^2(n+5)\left(n^2-3\right)x_p^{n+3}}{16(n+2)^2(n+3)}-\frac{315\left(n^7+10n^6+24n^5-32n^4-133n^3+22n^2+156n-24\right)x_p^{n+4}}{32(n+2)^2(n+3)(n+4)}$$
$$-\frac{315(n+1)\left(n^4+4n^3-5n^2-18n+12\right)x_p^{n+5}}{16(n+2)(n+3)(n+4)}+\frac{315(n+1)^2\left(n^4+4n^3-5n^2-18n+12\right)x_p^{n+6}}{32(n+2)(n+3)(n+4)}+\frac{315n^2\left(n^2-3\right)^2x_p^{2n+4}}{32(n+2)^2}$$
$$-\frac{315\left(4n^9+20n^8-n^7-123n^6-95n^5+211n^4+185n^3-99n^2-48n+18\right)x_p^{2n+5}}{16(n+2)^2(n+3)(2n+1)(2n+5)}$$
$$\left.+\frac{315n(n+1)\left(n^2-3\right)\left(n^4+4n^3-5n^2-18n+12\right)x_p^{2n+6}}{32(n+2)^2(n+3)(n+4)}\right)-I_5 \qquad \text{(C1)}$$

where $I_5=\int_0^1 f_{1t}\,u\,dx$ is evaluated using *Mathematica* and data required from this part for plotting the graphs is obtained directly from *Mathematica*.